Uni GH Essen preprint
January 24, 2000

Polymerized Membranes, a Review

Kay Jörg Wiese*

Fachbereich Physik, Universität GH Essen, 45117 Essen, Germany

Abstract

Membranes are of great technological and biological as well as theoretical interest. Two main classes of membranes can be distinguished: Fluid membranes and polymerized, tethered membranes. Here, we review progress in the theoretical understanding of polymerized membranes, i.e. membranes with a fixed internal connectivity. We start by collecting basic physical properties, clarifying the role of bending rigidity and disorder, theoretically and experimentally as well as numerically. We then give a thorough introduction into the theory of self-avoiding membranes, or more generally non-local field theories with δ-like interactions. Based on a proof of perturbative renormalizability for non-local field-theories, renormalization group calculations can be performed up to 2-loop order, which in 3 dimensions predict a crumpled phase with fractal dimension of about 2.4; this phase is however seemingly unstable towards the inclusion of bending rigidity. The tricritical behavior of membranes is discussed and shown to be quite different from that of polymers. Dynamical properties are studied in the same frame-work. Exact scaling relations, suggested but not demonstrated long time ago by De Gennes for polymers, are established. Along the same lines, disorder can be included leading to interesting applications. We also construct a generalization of the $O(N)$-model, which in the limit $N \to 0$ reduces to self-avoiding membranes in analogy with the $O(N)$-model, which in the limit $N \to 0$ reduces to self-avoiding polymers. Since perturbation theory is at the basis of the above approach, one has to ensure that the perturbation expansion is not divergent or at least Borel-summable. Using a suitable reformulation of the problem, we obtain the instanton governing the large-order behavior. This suggest that the perturbation expansion is indeed Borel-summable and the presented approach meaningful. Some technical details are relegated to the appendices. A final collection of various topics may also serve as exercises.

PACS numbers: 05.70.Jk, 11.10.Gh, 64.60.Ak, 75.10.Hk

Review to be published in volume 19 of Domb Lebowitz,
Phase Transitions and Critical Phenomena.

Habilitation thesis, Fakultät für Physik, Universität GH Essen, Germany
submitted May 21, 1999; accepted October 20, 1999

*Email: wiese@next23.theo-phys.uni-essen.de

Contents

1 Introduction and outline

One of the most challenging ideas in modern physics is the concept of universality: Certain properties of physical systems do not depend on microscopic details and furthermore are equivalent for seemingly unrelated problems. This is epitomized by systems undergoing symmetry breaking continuous phase transitions. The most powerful tools to reveal these relations are delivered by quantum field theory, which has celebrated an overwhelming success in nearly all areas of physics. The study of the $O(N)$-model, which is a field theory for the statistics of N-component spins with short-range interactions, has shown that their critical behavior is described by a set of exponents which are completely characterized by the dimension and the underlying symmetry (the number of components of the order parameter). Universality is ensured since the microscopic details are averaged out, and do not affect the large scale fluctuations. A variety of techniques have been developed to examine the critical behavior of this model; possibly the most successful one is the renormalization group procedure [2] which analytically justifies the concept of universality. The technically most convenient implementations are field theoretical methods, e.g. the ε-expansion about the upper critical dimension of 4, an expansion about the lower critical dimension of 2, and exact re-summations in the large N limit. (For an review of these techniques, see Ref. [3].) The best studied method is the ε-expansion about the upper critical dimension of 4, where calculations have been performed up to fifth order. Together with resummation techniques which take care of the large-order behavior known from instanton calculus, this is a very powerful tool for extracting critical exponents.

On the other hand, field theories have strong connections to geometrical problems involving fluctuating lines. For example, the motion of particles in space-time describes a world-line. Summing over all world-lines, weighted by an appropriate action, is the Feynman path integral approach to calculating transition probabilities, which can alternatively be obtained from a quantum field theory. The latter can be extended to string theory, generalizing the sum over particle trajectories to the sum over trajectories of lines. Another example is the high-temperature expansion of the Ising model. The energy-energy correlation function can be expressed as a sum over all self-avoiding closed loops which pass through two given points. Self-avoidance is necessary in order not to overcount configurations. We face an important new theoretical concept, which is the subject of this review: Parameterizing the loop by its length, different parts of the loop interact with each other irrespective of their distance. Treating such phenomena in the framework of field-theory demands an enlargement of the concept of local field-theories to *multi-local ones*. The

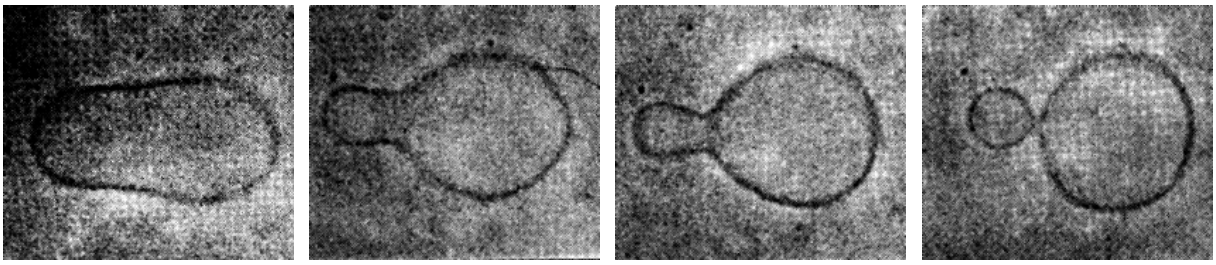

Figure 1.1: Budding of fluid membranes, from [1].

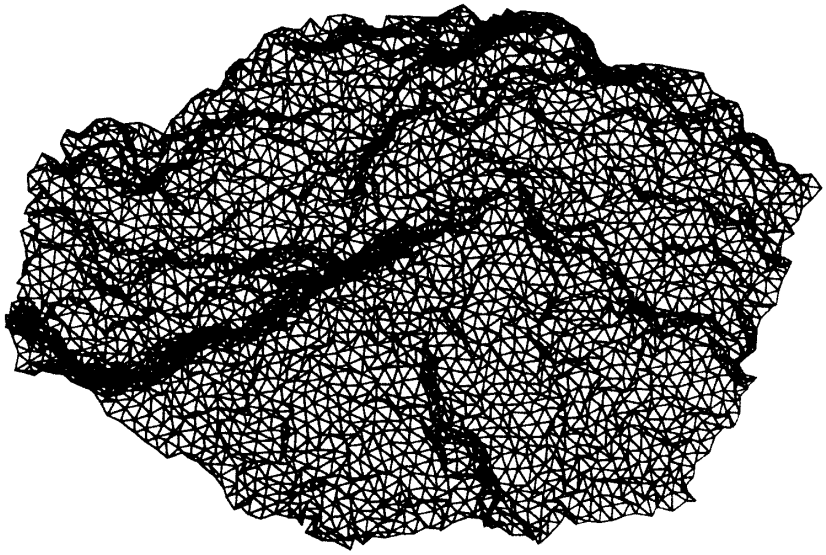

Figure 1.2: Polymerized tethered membrane in the flat phase, from [16].

first direct such approach was developed in the context of self-avoiding polymers, which are formally equivalent to the loops appearing in the high-temperature expansion of the Ising model, by Edwards and Des Cloizeaux [4–6]. In this approach, hard self-avoidance is replaced by a soft short range repulsive interaction upon contact of the monomers. This interaction is then studied perturbatively by expanding about ideal random walks. Here too, the perturbative expansion can be reorganized into an expansion about the upper critical dimension of 4, which was shown [7] to be equivalent to the perturbation expansion of ϕ^4-theory in the limit $N \to 0$. This equivalence provides two apparently different approaches for calculating the same exponents.

There is much work in the field theory community on generalizing results for fluctuating lines to entities of other internal dimensions D. The most prominent example is string theory, which describes $D = 2$ world sheets [8–11]. An earlier example is provided by the correspondence between gauge theories and random surfaces [12,13]. The low temperature expansion of the Ising model in d dimensions also results in a sum over surfaces that are $d - 1$ dimensional. For $d = 3$, the surfaces are made out of plaquettes, the basic objects of lattice gauge theories. All these objects share the common property that not only fluctuations of shape but also topology changes occur and have to be summed over in the partition function. The biologically relevant representatives of this class of membranes are fluid membranes, which in general are formed by a lipid bi-layer. I contrast to fluid membranes are "tethered", polymerized surfaces [14,15], which have a fixed internal connectivity, and are thus simpler than their fluid counterparts. Experimental realizations are e.g. the network formed by spectrin in red blood cells or graphite mono-layers. These systems may be found in three quite different phases: a collapsed compact phase, a flat phase and an intermediate crumpled swollen phase with fractal dimension of about 2.4. Experimentally, the situation is still under debate (cf. section 2.5). In numerical simulations (cf. section 2.5), generically flat membranes are found (see figure 1). The reason why eventually no crumpled swollen phase may be observable is that the rigidity of

tethered membranes is – in sharp contrast to fluid membranes – strongly enhanced by the effect of shear waves. Technically, integrating out these degrees of freedom renormalizes the rigidity, and if the initial rigidity is beyond a certain threshold, the membrane will become flat (see section 2.4). Intuitively this is analogous to a crumpled sheet of paper, which is much more rigid than an uncrumpled one.

Numerically, it has been observed that tethered membranes seemingly are always flat, even when starting with self-avoidance only. This can be traced back to the effective (entropic) bending rigidity which is always present in these models. However, since the largest membranes simulated so far consist of only 75×75 atoms in the simplest spring and bead model, which has the inconvenience of being rather rigid, and of about 25×25 atoms in the more sophisticated plaquette-models, simulations are far form being conclusive. These general physical, including numerical and experimental considerations are presented in more detail in section 2.

For theoretical analysis, it is convenient to further generalize to membranes of arbitrary (inner) dimension D, interpolating between polymers for $D = 1$ and membranes for $D = 2$. Simple power counting indicates that self-avoidance is relevant only for dimensions $d < d_c = 4D/(2-D)$, making possible an $\varepsilon = 2D - d(2-D)/2 \sim (d_c(D) - d)$-expansion, which was first carried to 1-loop order about an arbitrary point on the line $\varepsilon = 0$ in Refs. [17–21]. To obtain results for polymers or membranes, one then has the freedom to expand about *any* internal dimension D, and the corresponding upper critical dimension of the embedding space [22]. This freedom can be used to optimize the calculation of critical exponents.

A major breakthrough in the understanding of these non-local field theories is the proof by David, Duplantier and Guitter, that the field-theory of a D-dimensional self-avoiding tethered membrane is renormalizable to all orders in perturbation theory. The main technical tool is the multilocal operator product expansion (MOPE), generalizing the concept of (local) operator product expansion (OPE), introduced into field theory long time ago by Wilson [23] and Kadanoff [24], to the multilocal situation. We shall present this technique in section 3. A collection of useful tools is given in section 4, and a condensed version of the above-mentioned proof in section 5.

These general arguments have been checked by explicitly going to 2-loop order [25,26]. The calculation is technically difficult but it is valuable to understand the underlying principles. We therefore review these calculations in section 6, suggesting to the reader more concerned with applications to skip this section as well as section 5 with the discussion of the proof of perturbative renormalizability. The most important physical prediction of this calculation is that there exists a crumpled swollen phase with fractal dimension of about 2.4.

Another important question is whether non-leading terms play a role for the critical behavior of tethered membranes. This is certainly the case at the tricritical point, which separates the crumpled swollen from the compact phase, and which is analyzed in section 9. In contrast to polymers, whose tricritical behavior is dominated by the 3-point self-repulsion (which formally punishes triple intersection of the polymer with itself), in the case of the membrane ($D = 2$), this role is played by a modified 2-point interaction, not proportional to a δ-interaction, but to its second derivative [27]. Subdominant operators may also play a role at the self-avoiding fixed point, at finite ε, i.e. well below the upper

critical dimension [28].

It is well known that different dynamical models can lead to the same static behavior [29]. In the case of polymers, people have paid most attention to purely diffusive dynamics (Rouse model, model A) eventually including the effect of hydrodynamics (Zimm model). For a long time, the question whether these dynamical models are renormalizable, stayed open. As discussed in section 11, the methods mentioned above finally allowed to settle this question [30,31].

Somehow surprisingly, the same kind of model also applies to the dynamics of an extended elastic object, be it a polymer or a membrane, in quenched disordered. Technically, averaging over disorder generates non-local interactions on the polymer, with interactions proportional to the disorder correlations. The latter may be taken to be δ-distributions. In this respect, it is worth recalling that self-avoidance can also be generated by averaging over all realizations of an (imaginary) random potential, in which the polymer or membrane is fluctuating. In section 12, we review the analysis of a D-dimensional membrane (with $D = 0$ for a particle, $D = 1$ for a polymer and $D = 2$ for a membrane), in a quenched random force field with both potential and non-potential parts. In contrast to the pure potential case, this situation is accessible perturbatively [32,33].

As is well-known, string theory is defined as the sum over all closed manifolds with arbitrary topology. Excluding from this sum self-intersecting configurations is a formidable task beyond current technical capabilities. For polymerized membranes, i.e. with non-fluctuating metric, this sum can indeed be taken, generalizing the high temperature expansion of the $O(N)$-model mentioned above from a gas of self-avoiding loops of fugacity N, to a similar gas of closed fluctuating manifolds of internal dimension D [34,35]. As will be discussed in section 13, this generalization is not unique, leaving space for adaptation of the model to the situation in question. Among others, the model contains a novel mechanism not present in standard field theory, which turns first order transitions into second order ones ("reverse Coleman-Weinberg mechanism"). The model further contains a 1-loop fixed point for the random bond Ising model and finally allows for an intriguing conjecture regarding the nature of droplets dominating Ising criticality.

So far, these models have only been treated via perturbative techniques. An important question is, whether the theory is meaningful beyond perturbation expansion. This is a difficult issue, which so far is only partially answered for the case of self-avoiding polymers. A little bit easier to answer is the question, whether the perturbative series is well defined. For the case of the $O(N)$-model, it has been shown by Lipatov [36,37], that the series is divergent, but can be resummed using a Borel-transform. For tethered membranes, the situation is difficult, since the usual instanton methods do not apply. In section 14 we show, what the analog of the instanton for the ϕ^4-theory is, and why this implies that the perturbation series is also Borel-summable [38].

Finally let us point out that even though the primary aim of this review is to present from a unified viewpoint the theoretical concepts of multilocal field-theories, an effort is made to motivate the physical models and experimental relevance. On the other hand, the real progress which goes beyond today's interest, lies in the fundamental technical achievements, and the author feels that skipping technically important details, would render this review much less useful. In order to keep the text readable, the central ideas are given before embarking on technical calculations, and wherever this is possible, we

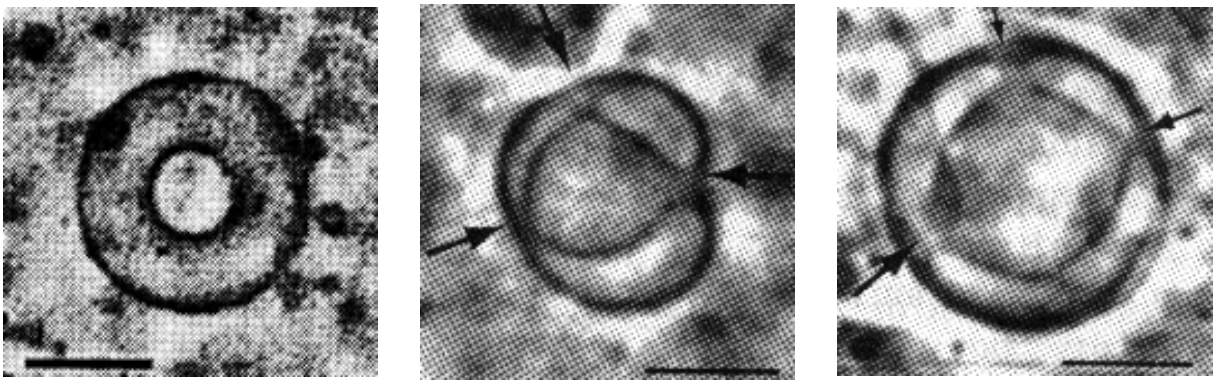

Figure 2.1: Fluid membranes with higher topology. From left to right: a 1-torus [39] and a 2- and 4-torus [40].

try to sketch how the techniques developed will be useful later.

The general structure of this review is therefore organized so that relevant material, which is necessary to place the following more technical parts in the physical context, is collected in section 2. The next section is devoted to the necessary elementary technical tools. The following sections are more specialized and can mostly be read independently, only necessitating section 3, and eventually 4.

2 Basic properties of membranes

2.1 Fluid membranes

Let us start by characterizing the different possible types of membranes. One very popular class of membranes are fluid membranes. We all know of soap-bubbles from childhood days. Biologically more relevant are bilayers of lipid molecules that are composed of a hydrophilic head and two hydrophobic chains. As shown in figure 2.2, in water the hydrophobic chains group together and form a lipid bilayer. This is the basis of most of the biologically relevant membranes.

For an analytical description, one needs the coordinate $\vec{r}(x)$ of the membrane as a function of an internal parameter x, characterized by the mapping

$$\vec{r} : x \in \mathbb{R}^2 \longrightarrow \vec{r}(x) \in \mathbb{R}^d \tag{2.1}$$

and by the induced metric

$$g_{\alpha\beta} = \partial_\alpha \vec{r} \partial_\beta \vec{r} \; . \tag{2.2}$$

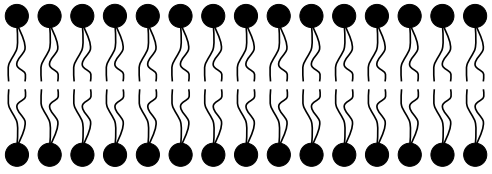

Figure 2.2: Model of a fluid membrane: Bilayer of lipid molecules that are composed of a hydrophilic head and two hydrophobic hydrocarbon chains.

We are now looking for the statistical weight of a membrane configuration. Since the lipid molecules in the membrane are free to move around, the energy, i.e. "Hamiltonian" of the membrane has to be invariant under coordinate transformations. This is achieved by the Canham-Helfrich Hamiltonian [41,42]

$$\mathcal{H}[\vec{r}] = \int \mathrm{d}^2x \, \sqrt{g(x)} \left[\tau + \frac{\kappa}{2} \left(H(x) - H_0 \right)^2 \right] \ . \tag{2.3}$$

$\mathrm{d}^2x \, \sqrt{g}$ is the invariant volume-element of the membrane, τ its surface tension, and κ the bending-rigidity, which is coupled to the square of the mean curvature

$$H = \frac{1}{2} \left(\frac{1}{R_1} + \frac{1}{R_2} \right) \ , \tag{2.4}$$

where R_1 and R_2 are the two curvature radii. H_0 is a spontaneous curvature, present in the case of symmetry breaking between the two sides of the membrane. Physically, rigidity is explained by the finite thickness of the membrane. RG-calculations indicate that bending-rigidity should be irrelevant at large distances [43,44]; this however has recently been criticized in [45].

Experimentally, fluid membranes offer a wide range of interesting and complex phenomena. Let us only mention the budding of a fluid membrane, as given in figure 1.1 and the appearance of higher genus objects (figure 2.1).

For a general review about fluid membranes, see [44,46–48].

Interestingly, the Hamiltonian (2.3) with $\kappa = 0$ also plays a central role in string theory. Here, one of the inner coordinates $\vec{x} = \binom{x_1}{x_2}$ is identified as $i \times$ time, and the other one as length on the string. Eq. (2.3) is then the action generating the motion of the string. Further generalizations use a metric $g_{\alpha\beta}$ independent of the imbedding space [8,49,9–11]. Strings are considered as one of the most promising candidates for unifying all fundamental interactions.

2.2 Tethered (polymerized) membranes

In this review, we shall concentrate on another class of membranes, which have a fixed and constant internal metric:

$$g_{\alpha\beta} = \delta_{\alpha\beta} \ . \tag{2.5}$$

These membranes have not yet found applications in high-energy physics, but are realized in experiments (see section 2.5). They are either called solid, tethered or polymerized membranes.

A microscopic model is given by the so-called "spring and bead model" (see figure 2.3), which consists of balls (beads) which are connected by springs and form a regular lattice. The model membrane is called "self-avoiding" since the beads cannot intersect each other. We will discuss Monte-Carlo simulations of this model in section 2.6.

A simpler situation occurs when self-intersections are allowed ("phantom-membrane"). Simulations as well as renormalization group calculations [50,51] indicate that such a membrane is crumpled for weak bending rigidity, $\kappa < \kappa_c$ and flat for $\kappa > \kappa_c$. At the phase-transition point $\kappa = \kappa_c$, the membrane is in another critical (or more precisely

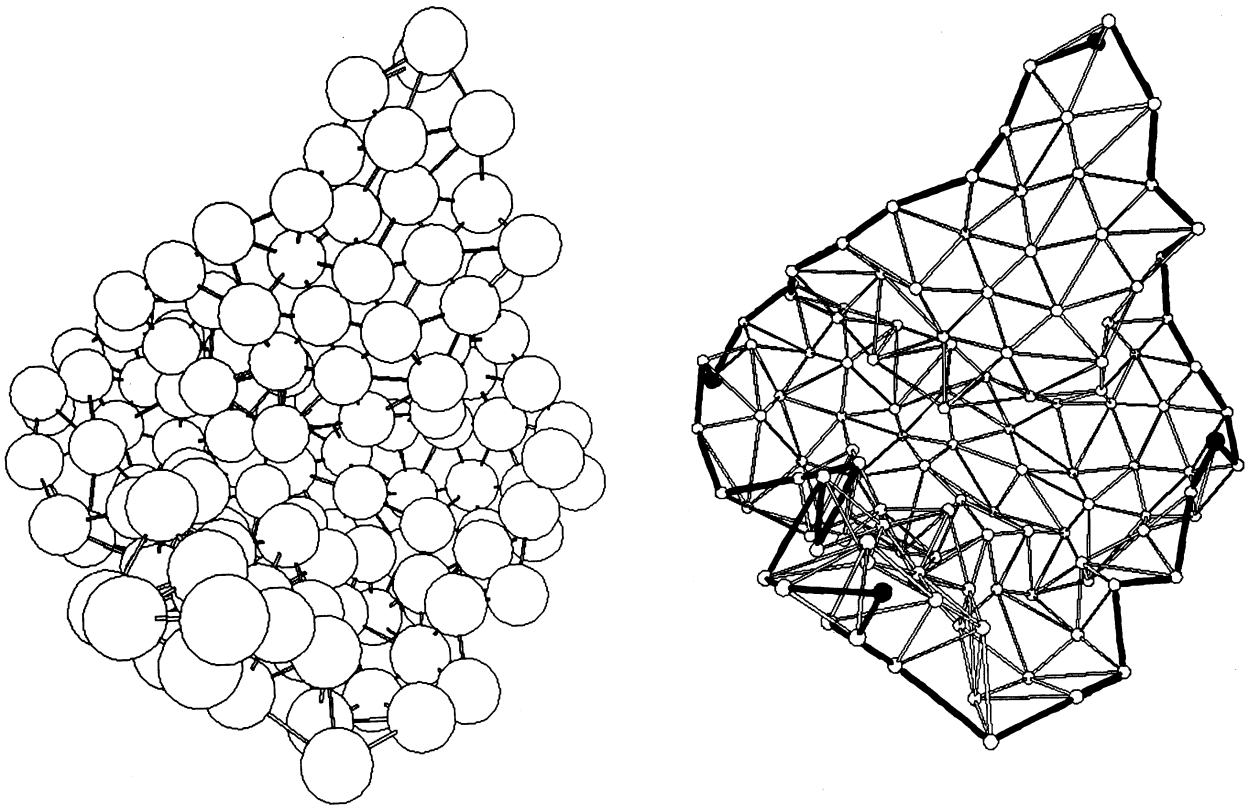

Figure 2.3: A tethered membrane (spring and bead model), from [15].

tricritical) state with a fractal dimension $d_{\rm f}$ in between the dimensions of the crumpled and flat phases. A mean-field treatment of this so-called "crumpling transition" is given in section 2.3. Contrary to intuition, the flat phase is not destroyed by fluctuations. This is demonstrated in section 2.4, where also the tricritical state at $\kappa = \kappa_c$ is discussed. On the other hand, in the small-rigidity phase, phantom-membranes will have a fractal dimension of infinity. For physical (self-avoiding) membranes which can not intersect themselves, this is clearly impossible, and one expects the physical bound

$$d_{\rm f} \leq d \tag{2.6}$$

induced by self-avoidance.

A continuous model to describe a self-avoiding membrane is

$$\mathcal{H}[\vec{r}] = \int \mathrm{d}^D x \, \frac{1}{2} \left(\nabla \vec{r}(x)\right)^2 + \frac{\mathfrak{b}}{2} \int \mathrm{d}^D x \int \mathrm{d}^D y \, \delta^d(\vec{r}(x) - \vec{r}(y)) \ . \tag{2.7}$$

It has first been proposed by Edwards [4] to describe polymers ($D = 1$). In that case, it is equivalent to scalar ϕ^4-field theory in the limit of $N = 0$ components [7]. In 1986 the model has been generalized to membranes ($D = 2$), independently by Kardar and Nelson [17,18] and by Aronovitz and Lubensky [19]. They observed that a direct calculation at $D = 2$ is impossible, but that one can make an analytic continuation from $D < 2$.

In contrast to polymers, with their equivalence to scalar field-theory, renormalization is *not* evident. At leading order, renormalizability has been verified by Duplantier, Hwa

and Kardar in 1990 [52]. For the general case, an important step was achieved by David, Duplantier and Guitter [53,54] who showed renormalizability of the theory

$$\mathcal{H}[\vec{r}] = \int \mathrm{d}^D x \, \frac{1}{2} \left(\nabla \vec{r}(x)\right)^2 + \mathfrak{g} \int \mathrm{d}^D x \, \delta^d(\vec{r}(x)) \ , \tag{2.8}$$

which describes a phantom (non self-avoiding) membrane in interaction with a single point (an impurity). The proof is based on a generalization of the forest algorithm introduced by Zimmermann [55] to δ-like interactions. Their last step was to prove the renormalizability of the full model [56,57], which we shall describe in section 5.

To extract numerical predictions from the ε-expansion is a tedious task. One of the problems is that since one cannot start from $D = 2$, an analytic continuation has to be performed starting at any point (D, d) on the critical curve, which will be defined in section 3.1. The first calculations which tried to fix the expansion-point via a minimal sensitivity scheme at 1-loop order were performed in [22]. The result of $d_{\mathrm{f}} \approx 3.5$ for membranes in 3 dimensions even violated the geometric bound of 3 discussed above. It became therefore necessary to perform 2-loop calculations, not only to test the renormalization proof, but also to obtain more reliable values for the fractal dimension. This task was accomplished in [25,26], and we review the main steps in section 6. For membranes in 3 dimensions these calculations predict a fractal dimension of about 2.4, eventually seen in some experiments and numerical simulations, see sections 2.5 and 2.6.

It is interesting to note that the model (2.7) can also be used to study self-avoiding fractal objects like Sierpinsky gaskets [58]. (But attention: One has to be careful in distinguishing the fractal and the spectral dimensions of the membrane.)

Let us mention still another class of membranes, namely hexatic membranes. They play an intermediate role between tethered and fluid membranes. For a review see [46] and [59–61].

In the rest of this section, we review some simple arguments for tethered membranes, as well as experiments.

2.3 Crumpling transition, the role of bending rigidity, and some approximations

Let us start by studying the different terms appearing in a mean-field description of membranes. Let

$$\vec{r} : x \in \mathbb{R}^D \ \longrightarrow \ \vec{r}(x) \in \mathbb{R}^d \tag{2.9}$$

be the coordinates of a D-dimensional manifold embedded into a d-dimensional space. For $D = 1$, this represents a polymer, for $D = 2$ a membrane. Suppose that the underlying lattice is regular and that after integration over the fast degrees of freedom the effective model becomes translationally invariant. An expansion à la Landau then leads to an effective free energy or "Hamiltonian" [62]

$$\begin{aligned} \mathcal{H}\left[\vec{r}(x)\right] = \int \mathrm{d}^D x \, \frac{\kappa}{2} (\partial_\alpha \partial_\alpha \vec{r})^2 + \frac{t}{2} \left(\partial_\alpha \vec{r}\right)^2 + \mathfrak{u} \left(\partial_\alpha \vec{r} \partial_\beta \vec{r}\right)^2 + \mathfrak{v} \left(\partial_\alpha \vec{r} \partial_\alpha \vec{r}\right)^2 \\ + \frac{\mathfrak{b}}{2} \int \mathrm{d}^D x \int \mathrm{d}^D y \, \delta^d(\vec{r}(x) - \vec{r}(y)) \ . \end{aligned} \tag{2.10}$$

The last term, a self-repulsion upon contact, is a non-local interaction in the internal coordinates x, but local in the membrane position $\vec{r}(x)$. The local terms are the different

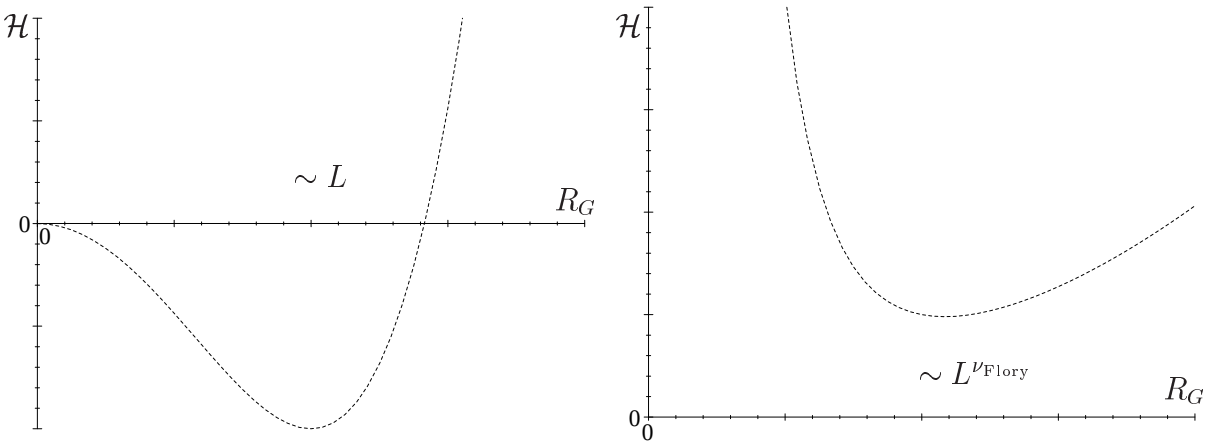

Figure 2.4: Free energy for $t < 0$ (left) and $t > 0$ (right) in the limit of large membranes.

contributions to the elastic energy. The coefficients t, $\mathfrak{u}$ and $\mathfrak{v}$ weight the elastic and inelastic harmonic energies, whereas κ measures the bending-rigidity.

The analogy to the usual ϕ^4-theory becomes apparent upon identifying the tangents $\vec{t}_\alpha := \partial_\alpha \vec{r}$ as order-parameter. However, this analogy is only valid at the mean-field level, and will be destroyed by fluctuations. Mean-field theory suggests a phase-transition at $t = 0$, where the parameter t is equal to $T - T_c$, the difference in temperature T to the critical temperature T_c.

At high temperature, t is positive due to entropy and the correlation between the tangential vectors decays exponentially fast. The membrane is in a crumpled phase.

For negative t, the terms proportional to $(\partial r)^4$ restore positivity of the action, provided that $\mathfrak{u} + \mathfrak{v} > 0$ and $\mathfrak{u} + D\mathfrak{v} > 0$. The symmetry is spontaneously broken, and the order-parameter $\vec{t}_\alpha$ has a non-zero expectation value, of the form $\vec{t}_\alpha = \zeta \vec{\mathbf{e}}_\alpha$, where $\vec{\mathbf{e}}_\alpha$ is a set of orthonormal base vectors. At zero temperature, the membrane is in a flat (ordered) phase, with

$$\zeta = \frac{1}{2}\sqrt{\frac{|t|}{\mathfrak{u} + D\mathfrak{v}}} \ . \tag{2.11}$$

This resembles the XY-model in 2 dimensions. There, long-range order is destroyed by spin-waves. We shall see in the next section, that fluctuations renormalize the rigidity of the membrane and render it stiffer. This renormalization is sufficient to make the membrane flat. For further discussion of the thermodynamic behavior see [63].

To incorporate self-avoidance, let us use the Flory-approximation. This consists in replacing $\vec{r}(x)$ by the radius of gyration R_G and derivatives with respect to x by $1/L$, as well as the integration over x by L^D, where L is the size of the flat membrane. This leads (up to numerical factors) to

$$\mathcal{H} \approx \kappa L^{D-4} R_G^2 + t L^{D-2} R_G^2 + (\mathfrak{u} + D\mathfrak{v})\, L^{D-4} R_G^4 + \mathfrak{b} L^{2D} R_G^{-d} \ . \tag{2.12}$$

First of all, the bending-rigidity κ can always be neglected with respect to t and $\mathfrak{u}$.

For $t < 0$ and in the physical region ($D \leq d$), the terms proportional to t and $\mathfrak{u} + D\mathfrak{v}$ dominate and minimizing the free energy leads to

$$R_G \sim L \ . \tag{2.13}$$

Self-avoidance can be neglected at large scale.

For $t > 0$, self-avoidance prevents the membrane from collapsing, and balancing the terms of order t and $\mathfrak{b}$ gives

$$R_G \sim L^{\nu_{\rm Flory}} \tag{2.14}$$

with the Flory-exponent

$$\nu_{\rm Flory} = \frac{2+D}{2+d} \ . \tag{2.15}$$

We will show in section 7.5 that Eq. (2.15) is a reasonable approximation in the crumpled phase. In general we will find

$$R_G \sim L^{\nu^*} \tag{2.16}$$

with some non-trivial exponent ν^*.

Let us still mention the results for ν^* in the crumpled phase, obtained by a Gaussian variational approximation. We shall show in section 7.4 that this approximation becomes exact in the limit of $d \to \infty$ with probably exponentially small corrections. The work by Goulian [64], Le Doussal [65] and Guitter and Palmeri [66] predicts:

$$\nu_{\rm var} = \frac{2D}{d} \ . \tag{2.17}$$

For 2-dimensional membranes ($D = 2$), this differs from the Flory approximation by terms of order $1/d^2$.

2.4 Stability of the flat phase

In the last section, we saw that a simple scaling analysis suggests the existence of a flat phase. This phase could of course be destroyed by fluctuations. We shall show here that this is indeed the case for fluid membranes, but that a non-zero shear-modulus, i.e. a fixed connectivity, stabilizes the membrane in the flat phase [59].

Our presentation is largely inspired by the lecture of Nelson [67], but we will use an ϵ-expansion here instead of a self-consistent approximation.

To describe fluctuations of a membrane with inner coordinates $x = (x_1, x_2)$ around a flat configuration, it is advantageous to use the representation

$$\vec{r}(x_1, x_2) = \zeta \begin{pmatrix} x_1 + u_1(x_1, x_2) \\ x_2 + u_2(x_1, x_2) \\ h(x_1, x_2) \end{pmatrix} \ . \tag{2.18}$$

The line-element $\mathrm{d}\vec{r}$ is

$$\mathrm{d}\vec{r} = \zeta \begin{pmatrix} (1 + \partial_1 u_1)\,\mathrm{d}x_1 + \partial_2 u_1\,\mathrm{d}x_2 \\ \partial_1 u_2\,\mathrm{d}x_1 + (1 + \partial_2 u_2)\,\mathrm{d}x_2 \\ \partial_1 h\,\mathrm{d}x_1 + \partial_2 h\,\mathrm{d}x_2 \end{pmatrix} \ . \tag{2.19}$$

The deformation of this line-element is described by the deformation-matrix $u_{\alpha\beta}$ [68]

$$\mathrm{d}r^2 = \zeta^2 \left(\mathrm{d}^2 x + 2 u_{\alpha\beta}\,\mathrm{d}x_\alpha \mathrm{d}x_\beta \right) \ . \tag{2.20}$$

With the help of Eq. (2.19) we find:

$$u_{\alpha\beta} = \frac{1}{2}\left(\partial_\alpha u_\beta + \partial_\beta u_\alpha\right) + \frac{1}{2}(\partial_\alpha h)(\partial_\beta h) + \frac{1}{2}(\partial_\alpha u_\gamma)(\partial_\beta u_\gamma) \ . \tag{2.21}$$

The last term is of higher order in u and can be neglected in the following. (It has to be included at order ε^2.) We shall thus use

$$u_{\alpha\beta} \approx \frac{1}{2}\left(\partial_\alpha u_\beta + \partial_\beta u_\alpha\right) + \frac{1}{2}(\partial_\alpha h)(\partial_\beta h) \ . \tag{2.22}$$

The energy of a nearly flat membrane is the sum of bending-rigidity and deformation energy

$$\mathcal{H}\left[u,h\right] = \int \mathrm{d}^2x \, \frac{\bar{\kappa}}{2}\left(\Delta h\right)^2 + \frac{1}{2}\left[2\bar{\mu}u_{\alpha\beta}^2 + \lambda u_{\gamma\gamma}^2\right] \ . \tag{2.23}$$

$\bar{\mu}$ and λ are the Lamé-coefficients [68]. (We use $\bar{\mu}$ instead of the usual notation of μ [68] to reserve μ for the renormalization scale.) $\bar{\kappa}$, $\bar{\mu}$ and λ are related to κ, $\mathfrak{u}$ and $\mathfrak{v}$ by $\bar{\kappa} = \kappa\zeta^2$, $\bar{\mu} = 4\mathfrak{u}\zeta^4$ and $\lambda = 8\mathfrak{v}\zeta^4$.

In this expression, the displacement vector u_α appears only quadratic and can thus be eliminated by calculating its path-integral

$$\mathcal{H}_{\text{eff}}\left[h\right] = -k_B T \ln\left[\int D\left[u\right] \mathrm{e}^{-\mathcal{H}[u,h]/k_B T}\right] \ . \tag{2.24}$$

We separate in $u_{\alpha\beta}(x)$ the $(q=0)$-mode and use for the other modes the Fourier decomposition

$$u_{\alpha\beta}(x) = u_{\alpha\beta}^0 + A_{\alpha\beta}^0 + \sum_{q\neq 0}\left(\frac{i}{2}\left[q_\alpha \tilde{u}_\beta(q) + q_\beta \tilde{u}_\alpha(q)\right] + \tilde{A}_{\alpha\beta}(q)\right)\mathrm{e}^{iqx} \ , \tag{2.25}$$

where

$$\tilde{u}_\alpha(q) = \int \mathrm{d}^2x \, \mathrm{e}^{-iqx} u_\alpha(x) \tag{2.26}$$

and $\tilde{A}_{\alpha\beta}(q)$ is the Fourier transform of $A_{\alpha\beta}(x) = \frac{1}{2}\partial_\alpha h(x)\partial_\beta h(x)$:

$$\tilde{A}_{\alpha\beta}(q) = \frac{1}{2}\int \mathrm{d}^2x \, \mathrm{e}^{-iqx}\partial_\alpha h(x)\partial_\beta h(x) \ . \tag{2.27}$$

For $q \neq 0$, $\tilde{A}_{\alpha\beta}(q)$ is now decomposed into its longitudinal and transversal parts. (That this is indeed possible is shown in appendix A.3.)

$$\tilde{A}_{\alpha\beta}(q) = \frac{i}{2}\left[q_\alpha \tilde{\varphi}_\beta(q) + q_\beta \tilde{\varphi}_\alpha(q)\right] + P_{\alpha\beta}^{\mathrm{T}}(q)\tilde{\Phi}(q) \ , \tag{2.28}$$

where

$$P_{\alpha\beta}^{\mathrm{T}}(q) = \delta_{\alpha\beta} - \frac{q_\alpha q_\beta}{q^2} \tag{2.29}$$

is the transversal projector and

$$\tilde{\Phi}(q) = P_{\alpha\beta}^{\mathrm{T}}(q)\tilde{A}_{\alpha\beta}(q) \ . \tag{2.30}$$

We can now absorb the longitudinal part $\tilde{\varphi}_\beta(q)$ of $\tilde{A}_{\alpha\beta}(q)$ by shifting the variable $\tilde{u}_\alpha(q)$:

$$\tilde{u}_\alpha(q) \;\longrightarrow\; \tilde{u}_\alpha(q) - \tilde{\varphi}_\alpha(q) \;. \tag{2.31}$$

It remains to integrate over $\tilde{u}_\alpha(q)$. To this aim expand

$$\mathcal{T} := 2\bar{\mu}\,\tilde{u}_{\alpha\beta}(q)\tilde{u}_{\alpha\beta}(-q) + \lambda\,\tilde{u}_{\alpha\alpha}(q)\tilde{u}_{\beta\beta}(-q) \tag{2.32}$$

in the basis of rotational invariants q^2, $|q\tilde{u}(q)|^2$ and $\tilde{u}(q)\tilde{u}(-q)$:

$$\mathcal{T} = \bar{\mu}q^2|\tilde{u}(q)^2| + (\bar{\mu}+\lambda)|q\tilde{u}(q)|^2 + (2\bar{\mu}+\lambda)|\tilde{\Phi}(q)|^2 + \lambda\left(iq\tilde{u}(q)\tilde{\Phi}(-q) + \text{c.c.}\right) \;. \tag{2.33}$$

By a second variable-transformation

$$\tilde{u}_\alpha(q) \;\longrightarrow\; \tilde{u}_\alpha(q) + \frac{\lambda}{2\bar{\mu}+\lambda}\,\frac{iq_\alpha}{q^2}\,\tilde{\Phi}(q) \tag{2.34}$$

terms proportional to $\tilde{\Phi}$ and $\tilde{u}$ are decoupled and we obtain

$$\mathcal{T} = \frac{4\bar{\mu}(\bar{\mu}+\lambda)}{2\bar{\mu}+\lambda}\tilde{\Phi}(q)\tilde{\Phi}(-q) + \text{quadratic terms in } \tilde{u} \;. \tag{2.35}$$

Up to a constant, the effective Hamiltonian (2.24) thus becomes

$$\mathcal{H}_{\text{eff}}[h] = \frac{\bar{\kappa}}{2}\int \mathrm{d}^2x\,(\Delta h)^2 + \frac{\bar{K}}{2}\int' \mathrm{d}^2x\,\left(P^T_{\alpha\beta}\,[\partial_\alpha h(x)\partial_\beta h(x)]\right)^2 \;. \tag{2.36}$$

The "prime" indicates that the 0-mode is excluded from the integral. The coupling constant $\bar{K}$ is

$$\bar{K} = \frac{\bar{\mu}(\bar{\mu}+\lambda)}{2\bar{\mu}+\lambda} \;. \tag{2.37}$$

We see that the shear-modulus $\bar{\mu}$ is responsible for the interaction. For fluid membranes, $\bar{\mu} = 0$ and no correction appears, even if $\lambda \neq 0$.

We shall now study Eq. (2.36) in perturbation theory, by using an $\epsilon = 4-D$ expansion. A similar technique was employed by Aronovitz and Lubensky in [20], where they study the RG-flow for all fields. A self-consistent method was utilized in [59,67].

To carry out an ϵ-expansion, we rewrite the effective Hamiltonian (2.36) as

$$\mathcal{H}_{\text{eff}}[h] = \frac{Z}{2}\int \mathrm{d}^Dx\,(\Delta h)^2 + \frac{K}{2}Z_K\mu^\epsilon\int' \mathrm{d}^Dx\,\left(P^T_{\alpha\beta}\,[\partial_\alpha h(x)\partial_\beta h(x)]\right)^2 \;, \tag{2.38}$$

where $\bar{\kappa}$ has been absorbed into the field-normalizations ($h \to h/\sqrt{\bar{\kappa}}$) and

$$\begin{aligned} K_0 &= \frac{\bar{K}}{\bar{\kappa}^2} = K\frac{Z_K}{Z^2}\mu^\epsilon \\ h_0(x) &= \sqrt{Z}\,h(x) \;. \end{aligned} \tag{2.39}$$

The renormalization factors Z and Z_k absorb the divergences and are fixed by the minimal subtraction scheme. μ is the renormalization scale, $\epsilon = 4 - D$ the dimension of the bare coupling. Bare quantities are indexed as $_0$. The vertex is

$$\frac{K}{2} \times$$ 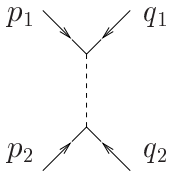

$$\times \frac{\delta^D(p_1 + p_2 + q_1 + q_2)}{(2\pi)^D} \prod_{i=1,2} \frac{(p^i q^i)^2 - (p^i)^2 (q^i)^2}{(p^i + q^i)^2} \ . \tag{2.40}$$

We shall now calculate perturbative corrections. As the 0-mode is excluded from the integration, the contribution to κ coming from the "tadpole" is 0:

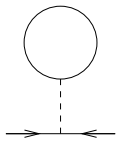 $= 0 \ .$ (2.41)

The second contribution to the renormalization of κ is:

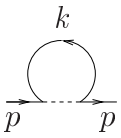

$$= \int_k \left(\frac{(pk)^2 - p^2 k^2}{(p+k)^2} \right)^2 \frac{1}{k^4} \ . \tag{2.42}$$

A divergence for $k \to \infty$ is manifest as a pole in $1/\epsilon$ with positive residue $\mathcal{C}$ (which needs not be specified):

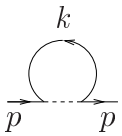

$$= (p^2)^2 \frac{\mathcal{C}}{\epsilon} p^{-\epsilon} \ . \tag{2.43}$$

The divergence of this diagram is subtracted at scale μ by choosing

$$Z = 1 - \frac{2\mathcal{C}}{\epsilon} K \ . \tag{2.44}$$

The sign is such that the interaction re-enforces the bending-rigidity. To analyze the renormalization of the vertex, we remark that due to the transversal projector, all three possible diagrams are convergent:

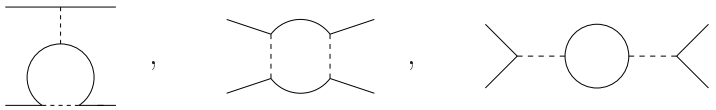 (2.45)

This is not evident from power-counting. Hence at 1-loop order

$$Z_K = 1 \ , \tag{2.46}$$

and renormalization becomes particularly simple. The function $\beta(K)$ and the full scaling dimension $\zeta(K)$ of the field h, the roughness-exponent, are obtained from Eq. (2.39) as

$$\beta(K) = \mu \frac{\partial}{\partial \mu}\bigg|_0 K = \frac{-\epsilon K}{1 + K \frac{\partial}{\partial K} \ln Z_K - 2K \frac{\partial}{\partial K} \ln Z} \tag{2.47}$$

$$\zeta(K) = \frac{4-D}{2} - \frac{1}{2} \mu \frac{\partial}{\partial \mu}\bigg|_0 \ln Z = \frac{4-D}{2} - \frac{1}{2} \beta(K) \frac{\partial}{\partial K} \ln Z \ . \tag{2.48}$$

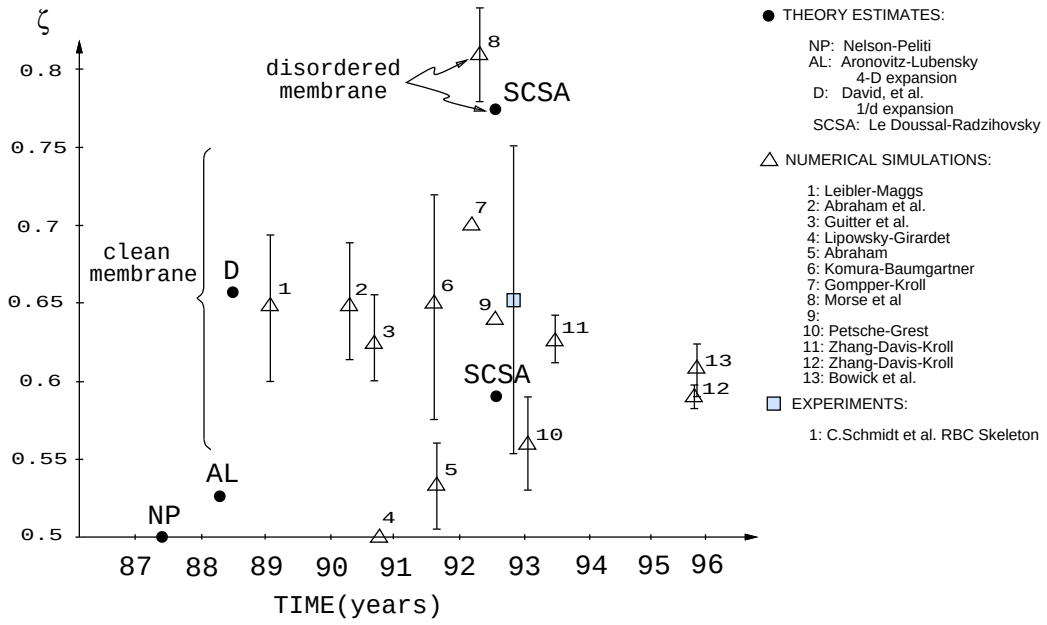

Figure 2.5: Estimates of the roughness-exponent ζ as a function of time. Courtesy of P. Le Doussal, with kind permission; figure by P. Le Doussal and L. Radzihovsky.

Since $\mathcal{C}$ is positive, the β-function possesses a positive, IR-stable fixed point at 1-loop order, which we denote K^*. Then

$$\zeta^* = \zeta(K^*) = \frac{4-D}{4} + O(\epsilon^2) \ . \tag{2.49}$$

(This result could have faster been obtained by using the method of exact exponent identities explained in section 3.9.) In $D = 2$

$$\zeta^* = \frac{1}{2} + O(\epsilon^2) \ . \tag{2.50}$$

This can be interpreted as an effective k-dependent bending-rigidity

$$\kappa_{\rm eff}(k) \approx \bar{\kappa}\frac{\mu}{k} \ . \tag{2.51}$$

We can now analyze the stability of the flat phase. Following De Gennes and Taupin [69], we estimate the fluctuations of the normal to the surface projected on x_3 (the component parallel to $h(x)$):

$$n_3(x) = \frac{1}{\sqrt{1+(\nabla h(x))^2}} \ . \tag{2.52}$$

The first term of the expansion is the mean of $(\nabla h(x))^2$. Without interaction ($K = 0$) it is:

$$\Big\langle (\nabla h(x))^2 \Big\rangle_0 = k_B T \int \frac{{\rm d}^2 q}{(2\pi)^2} \frac{q^2}{\bar{\kappa} q^4} \approx \frac{k_B T}{2\pi\bar{\kappa}} \ln(L/a) \ , \tag{2.53}$$

where L and a are IR and UV-cutoffs. As for many two-dimensional systems, the logarithmic divergence at large distances indicates that order is destroyed by fluctuations.

For membranes with non-zero shear-modulus, the estimate (2.53) is incorrect. One has to take care of the renormalization of κ, hence replace κ in Eq. (2.53) by $\kappa_{\text{eff}}(k)$, given by Eq. (2.51). This yields:

$$\left\langle (\nabla h(x))^2 \right\rangle_{\text{with } \kappa_{\text{eff}}} = k_B T \int \frac{\mathrm{d}^2 q}{(2\pi)^2} \frac{q^2}{\kappa_{\text{eff}}(q) q^4} = \text{IR-convergent} \ . \tag{2.54}$$

The normals keep their preferred direction parallel to x_3, even for systems with infinite size. The symmetry is broken and the membrane flat. This seems to be a violation of the Mermin-Wagner theorem: In fact, the fluctuations in the membrane give rise to long-range interactions, for which the Mermin-Wagner theorem is not valid.

To conclude: As soon as the membrane is in the phase of high bending-rigidity, i.e. the flat phase, the in-membrane fluctuations reinforce the bending-rigidity and stabilize the membrane. Stated differently: The fixed point of the flat phase is attractive.

Nevertheless, the fluctuations in the height h are large and described by a non-trivial roughness exponent ζ

$$\left\langle (h(x) - h(y))^2 \right\rangle \sim |x - y|^{2\zeta} \ . \tag{2.55}$$

This exponent was estimated above to be $\frac{1}{2}$. It can also be calculated by an expansion in $1/d$ [70], $\epsilon = 4 - D$ [50] or within a self-consistent screening approximation [71] and can be compared with experiments [72], and numerics [16,73–77]. This should rule out the value of $\zeta = \frac{1}{2}$, proposed in [78–80]. This is summarized in figure 2.5.

We have also mentioned above that the crumpling transition occurs at a critical value of the bending rigidity. This transition point is a different tri-critical state, accessible to renormalization-group treatments and numerics. The fractal exponent ν^* is then 0 in the crumpled phase, 1 in the flat phase, and at the crumpling transition given by the $1/d$-estimate [70,51]

$$\nu_{\text{c}}^* = 1 - \frac{1}{d} \ , \tag{2.56}$$

which agrees with numerical values in $d = 3$ [81,82]. See also [46,50,63,83–87].

Also see [88] for a study of the membrane elasticity at low temperatures and [89] for a stack of membranes.

2.5 Experiments on tethered membranes

Few experiments have been realized up to now. The most promising are:

- The spectrin-network of red blood cells forms a natural membrane, easily accessible experimentally [94,72]. The inconvenience of this system is the large intrinsic bending-rigidity which first has to be reduced. No experiment showing a crumpled phase has been done. In the flat phase, one finds an anomalous roughness exponent ζ of about $\zeta_{\text{flat}} \approx 0.6$ [72], as discussed at the end of the preceding subsection.

- 2-dimensional networks of polymers [95] seem to be promising. However, experimental measurements are missing. Recently, Rehage and coworkers have succeeded in producing sufficiently highly polymerized membranes [96] and experiments to find the fractal phase are planned [97].

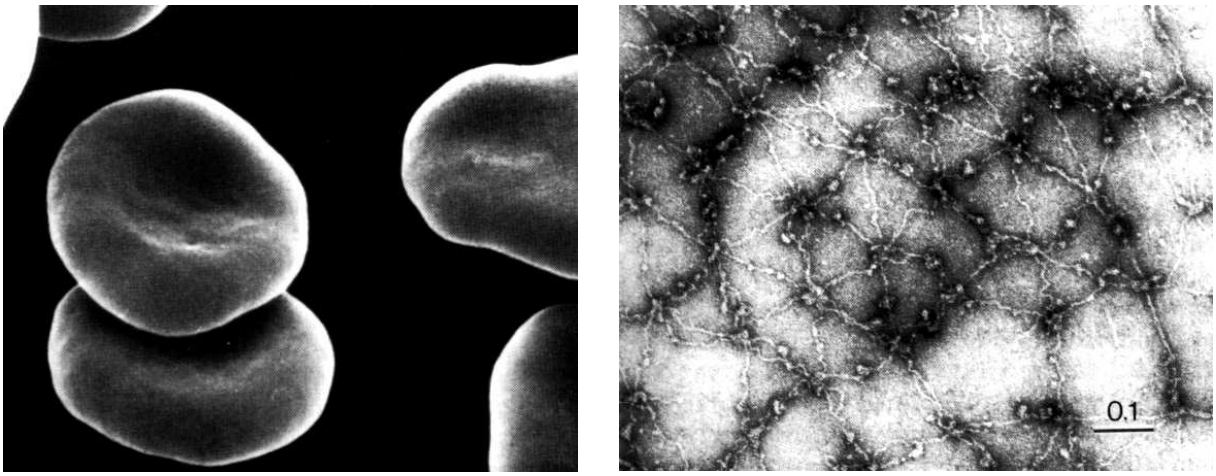

Figure 2.6: Image of a red blood-cell (left) and the underlying spectrin network (right) [90,91] from [92].

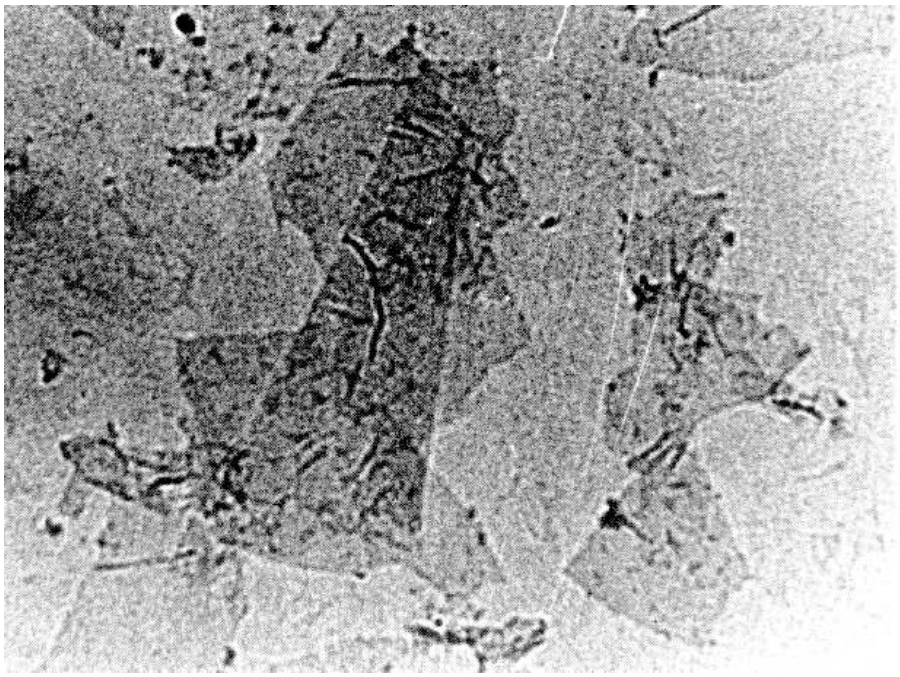

Figure 2.7: Image of a graphite membrane taken by a transmission electron microscope [93]. The linear dimension is about 1 micrometer.

- Molybdene disulfide (MoS_2) can be produced in extremely pure form. The experiments which we know of [98] find it in a strongly folded phase.

- Graphite oxide: For this material, experiments have been realized: Graphite is a layered material, and only very weak (van der Waals) forces exist between different layers. One therefore may cut out a piece of such a layer. By an exothermic reaction of graphite with some oxidant (the principle of black powder), one obtains a sample which consists of pieces of a single layer of graphite, decorated with oxygen-atoms at its border. One expects that these membranes have a very small bending-rigidity.

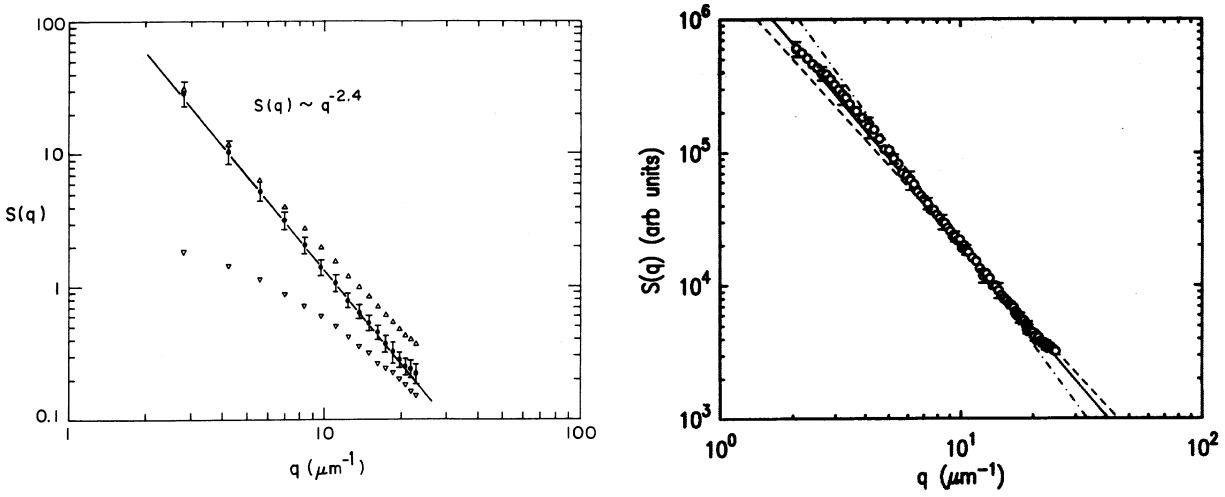

Figure 2.8: Static structure factor of graphite oxide membranes membranes in alkalic solution as function of the wave-vector q obtained from light-scattering in the visible domain. Taken from [93] (left) and [99] (right).

The first experiments undertaken by Hwa et al. [93] have shown such a crumpled phase with a fractal dimension near to the Flory results ($d_f = 2.5$) besides a collapsed and a flat phase. This was achieved by varying the concentration of H^+ of the dispersion. In later experiments by Spector et al. [99] this intermediate phase was no longer observed. The interpretation of these experiments is however not unambiguous. Extrapolating the light-scattering data of [93] reproduced on figure 2.8 predicts a fractal dimension of $d_f = 2.4$ whereas the very similar data of [99] lead to $d_f = 2.3$. However, based on a technique, where the sample is frozen ultra-fast, then cut into thin samples and analyzed via transmission electron microscopy, the authors of [99] were unable to see fractal objects and therefore concluded on the absence of a fractal phase. This debate certainly deserves further clarification. For more details see [100].

In summary: The experimental situation is not very transparent.

Let us still mention another very amusing class of experiments. Crunching a thin aluminum foil in the attempt to form a ball [101,102], also allows to measure a fractal dimension, which turns out to be very close to the Flory-result of Eq. (2.15). This result is easily reproduced on a table-top experiment with paper, see figure 2.9. However, since crunching aluminum foil is certainly a non-equilibrium process, this may be a coincidence.

2.6 Numerical simulations of self-avoiding membranes

In this section we review existing numerical simulations of tethered membranes. If not stated otherwise, these are membranes ($D = 2$) embedded into 3 dimensions.

The first simulations for self-avoiding membranes were performed for very small systems (121 beads) by Kantor, Kardar and Nelson [14,15] in 1986. They obtained $\nu^* = 0.80 \pm 0.05$ in agreement with the Flory-approximation. Here, as in most of the simulations, self-avoidance is effective between the beads (of finite size) of the network. There

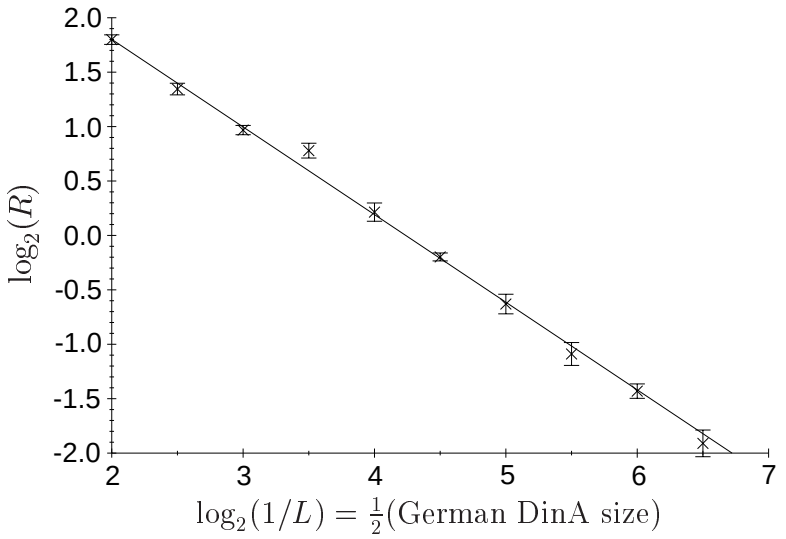

Figure 2.9: Result of crunching a sheet of paper of linear size L to a ball of diameter R. This leads to a fractal dimension of $d_{\rm f} = 2.4$, equivalent to $\nu^* = 0.82$.

exists thus a maximal angle smaller than π, by which the membranes can be folded. (For a visualization, see figure 2.3.)

As we discussed in section 2.4, phantom membranes show a crumpling transition induced by bending-rigidity. Shortly after this had been established numerically [81,82], an attempt was made to study this transition in the presence of self-avoidance [103–107]. The transition has completely disappeared and the membranes were always found flat for any (positive) value of the bending-rigidity. A simple explanation due to Abraham and Nelson [16] goes as follows: the simulated model consists out of beads (of finite size) and tethers linking the beads together. The tether-length is chosen such that the beads cannot penetrate through the holes left in-between. Then, the range of possible configurations is restricted and is re-interpreted as an effective bending-rigidity. This bending-rigidity was claimed responsible for the flat phase, following the scenario of the crumpling transition of a phantom membrane, induced by bending-rigidity.

The question therefore arises, whether the flat phase is an artifact of the simulations, or whether it is generic. Let us mention two simulations in this context: The first is due to Kantor and Kremer [108]. They studied the usual bead-and-tether model, but restricted self-avoidance on the membrane to a finite distance l. Since now the interaction is local, one can study the crumpling transition induced by the bending-rigidity σ. For $\sigma > \sigma_c$ a flat phase is found, whereas for $\sigma < \sigma_c$ the membrane is found in a crumpled state. Taking now the limit of large l, the value of the critical bending-rigidity σ_c scales to 0. They then concluded that this indicates that the flat phase persists down to $\sigma_c = 0$. It would be nice to have more extensive simulations available than the 169 to 331 beads studied there.

In another simulation, Liu and Plischke [109] have found an intermediate fractal phase by adding long-range *attraction*, and then adjusting the temperature. This intermediate phase was found for some range of temperature and membranes of up to 817 particles. In a similar simulation, Grest and Petsche [110] were also able to find this intermediate

phase, but only for a specific value of the temperature. This is not surprising from the renormalization-group point of view: Long-range forces are in general relevant operators, such that a fine-tuning is necessary to reach the critical point. Let us also mention another trick used in [110]: They rendered the membrane much more flexible by adding additional beads between the nodes of the lattice, forming the membrane.

A similar idea is to dilute the membrane by randomly cutting off links [111,112]. This attempt was not very fruitful: The flat phase persisted up to the percolation threshold.

The best numerical realization of tethered membranes is obtained by imposing self-avoidance not between beads but between the plaquettes forming the membrane. The first such simulation was carried out by Baumgärtner et al. [113,114], who indeed found the fractal phase. Within a very similar simulation, Kroll and Gompper [115] were not able to confirm these conclusions. A repetition of these simulations with larger systems as those studied there (up to 496 plaquettes) would be very much welcome to clarify the situation.

Other interesting simulations are for membranes in a 4-, 5-, 6- and 8-dimensional space. Grest found in [116] that membranes are flat in dimensions $d = 4$, but crumpled swollen in larger dimensions. Complementary simulations by Barsky and Plischke [117] confirm this conclusion. These simulations are in agreement with the value of ν^* predicted by the Gaussian variational ansatz, $\nu_{\text{var}} = 2D/d$ (see section 7.4), and larger than the 2-loop results (see figure 7.5 of page 86).

Remains to mention simulations on a Sierpinsky gasket with fractal dimension of about 1.585 and spectral dimension of about 1.356 [58]. As in the case of polymers, the results for $d = 3$ are in agreement with the Flory-approximation Eq. (2.15).

Also the folding transition of a membrane has been studied numerically [118].

Let us also mention studies of tethered membranes in confined geometries [119–121], of boundary effects [122], with negative bending-rigidity [123], of dynamics [124], and a couple of short reviews about the simulational aspects of tethered membranes [125,126].

2.7 Membranes with intrinsic disorder

A lot of publications have been devoted to the treatment of tethered (phantom) membranes with intrinsic disorder, including two-dimensional gels [71,111,127–144]. Let us give a brief summary of the main ideas, following the first publications [127–131]. Two kinds of disorder can be added. Since we are interested in the stability of the flat phase to such disorder, we study the Hamiltonian of a membrane in an expansion about a flat configuration, generalizing Eq. (2.23). We consider the general case of a D-dimensional membrane embedded in a d-dimensional space, such that

$$\vec{r}(x) = \zeta \begin{pmatrix} x_\alpha + u_\alpha(x) \\ h^j(x) \end{pmatrix} , \tag{2.57}$$

where $u(x) \in \mathbb{R}^D$ describes the D in-membrane (stretching) modes and $\vec{h}(x) \in \mathbb{R}^{d-D}$ the fluctuations in the $d - D$ transverse directions. The full Hamiltonian then reads in generalization of Eq. (2.23)

$$\mathcal{H}[u,h] = \int \mathrm{d}^D x \, \frac{\bar{\kappa}}{2} \left(\Delta \vec{h}\right)^2 + \frac{1}{2}\left[2\bar{\mu} u_{\alpha\beta}^2 + \lambda u_{\gamma\gamma}^2\right] + \sigma_{\alpha\beta}(x) u_{\alpha\beta}(x) + \vec{c}(x) \Delta \vec{h}(x) , \tag{2.58}$$

where we recall the definition of the deformation-matrix

$$u_{\alpha\beta} = \frac{1}{2}\left(\partial_\alpha u_\beta + \partial_\beta u_\alpha\right) + \frac{1}{2}(\partial_\alpha \vec{h})(\partial_\beta \vec{h}) + \frac{1}{2}(\partial_\alpha u_\gamma)(\partial_\beta u_\gamma) \ . \tag{2.59}$$

$\sigma_{\alpha\beta}(x)$ is a quenched random stress field, or variation of the metric. Microscopically it is due to different tether-lengths in the spring and bead model of figure 2.3. $\vec{c}(x)$ is a quenched random curvature field, favoring the mean curvature $\Delta\vec{h}(x)$, and breaking the reflection symmetry between the two sides of the membrane. It may be caused by a local difference in the chemical composition between the two sides of the membrane. The correlations are short ranged, of the form

$$\begin{aligned} \overline{\sigma_{\alpha\beta}(x)\sigma_{\gamma\delta}(x')} &= \left[\Delta_\lambda \delta_{\alpha\beta}\delta_{\gamma\delta} + 2\Delta_{\bar{\mu}}(\delta_{\alpha\gamma}\delta_{\beta\delta} + \delta_{\alpha\delta}\delta_{\beta\gamma})\right]\delta^D(x-x') \\ \overline{c^i(x)c^j(x')} &= \Delta_{\bar{\kappa}}\delta_{ij}\delta^D(x-x') \ . \end{aligned} \tag{2.60}$$

To study the renormalization group flow, the model is replicated, and the disorder averages are taken. This leads to an effective Hamiltonian similar to the pure model, but now with couplings between different replicas. One can then parallel the calculations of the pure model. The outcome is that at finite temperature, the long-wavelength properties of the membrane are unchanged. New physics emerges at or very near to zero temperature, characterized by a new non-trivial fixed point. Membranes with non-zero random spontaneous curvature are found in a flat phase with non-trivial critical exponents, analogous to the flat phase of the pure model at non-zero temperature [129–131]. This fixed point is accessible within an ε-expansion. Membranes with disorder in the metric are more difficult to access, since the fixed point lies outside the perturbatively accessible domain [127,128].

3 Field theoretic treatment of tethered membranes

3.1 Definition of the model, observables, and perturbation expansion

We start from the continuous model for a D-dimensional flexible polymerized membrane introduced in [19,17]. This model is a simple extension of the well known Edwards' model for continuous chains. The membrane fluctuates in d-dimensional space. Points in the membrane are labeled by coordinates $x \in \mathbb{R}^D$ and the configuration of the membrane in physical space is described by the field $r : x \in \mathbb{R}^D \longrightarrow r(x) \in \mathbb{R}^d$, i.e. from now on we note r instead of $\vec{r}$. In section 2.3 we had discussed that at high temperatures the free energy for a configuration is given by the (properly rescaled) Hamiltonian

$$\mathcal{H}[r] = \frac{Z}{2-D}\int\limits_x \frac{1}{2}(\nabla r(x))^2 + bZ_b\mu^\varepsilon \iint\limits_{x\ y} \tilde{\delta}^d(r(x)-r(y)) \ . \tag{3.1}$$

The so-called renormalization-factors Z and Z_b have the form $Z = 1 + O(b)$ and $Z_b = 1 + O(b)$; they will be explained later. The reader may safely set both to 1 for the moment. The integral $\int_x$ runs over D-dimensional space and ∇ is the usual gradient operator. The normalizations are

$$\int\limits_x := \frac{1}{S_D}\int \mathrm{d}^D x \ , \qquad S_D = 2\frac{\pi^{D/2}}{\Gamma(D/2)} \tag{3.2}$$

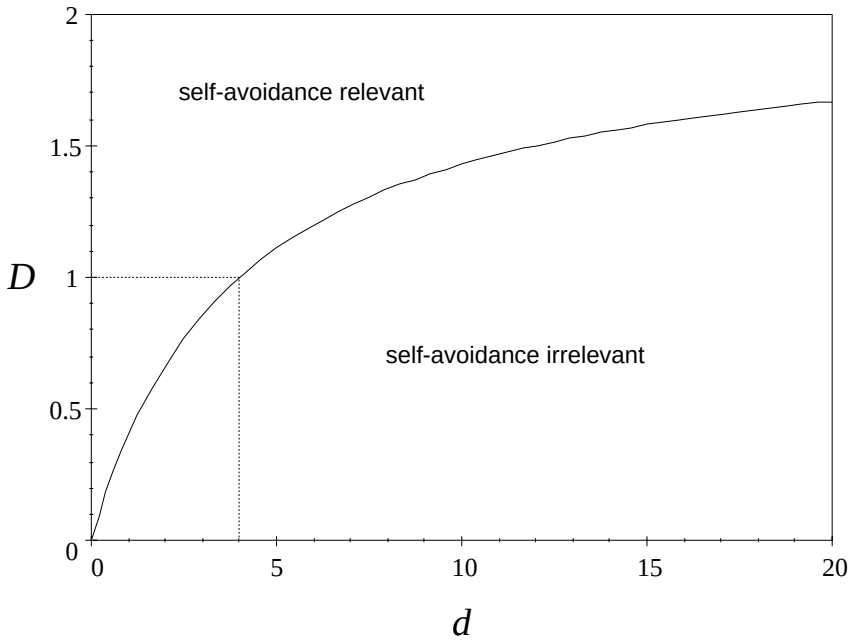

Figure 3.1: The critical curve $\varepsilon(D,d)=0$. The dashed line corresponds to the standard polymer perturbation theory, critical in $d=4$.

and

$$\tilde{\delta}^d(r(x)-r(y)) = (4\pi)^{d/2}\delta^d(r(x)-r(y)) \ . \tag{3.3}$$

The latter term is normally used in Fourier-representation

$$\tilde{\delta}^d(r(x)-r(y)) = \int\limits_p \mathrm{e}^{ip[r(x)-r(y)]} \ , \tag{3.4}$$

where the normalization of $\int_p$ is given by

$$\int\limits_p = \pi^{-d/2}\int \mathrm{d}^d p \tag{3.5}$$

to have

$$\int\limits_p \mathrm{e}^{-p^2 a} = a^{-d/2} \ . \tag{3.6}$$

All normalizations are chosen in order to simplify the calculations, but are unimportant for the general understanding. (They are collected in appendix A.1). μ is an internal momentum scale, such that μx is dimensionless. It is introduced to render the coupling b dimensionless. The first term in the Hamiltonian is a Gaussian elastic energy which is known to describe the free "phantom" surface. The interaction term corresponds (for $b>0$) to a weak repulsive interaction upon contact. The expectation values of physical observables are obtained by performing the average over all field-configurations $r(x)$ with the Boltzmann weight $e^{-\mathcal{H}[r]}$. This average can not be calculated exactly, but one can expand about the configurations of a phantom, i.e. non-interacting surface.

Such a perturbation theory is constructed by performing the series expansion in powers of the coupling constant b. This expansion suffers from ultraviolet (UV) divergences which have to be removed by renormalization and which are treated by dimensional regularization, i.e. analytical continuation in D and d. A physical UV-cutoff could be introduced instead, but would render the calculations more complicated. Long-range infrared (IR) divergences also appear. They can be eliminated by using a finite membrane, or by studying translationally invariant observables, whose perturbative expansion is also IR-finite in the thermodynamic limit (infinite membrane). Such observables are "neutral" products of vertex operators

$$\mathcal{O} = \prod_{a=1}^{N} \mathrm{e}^{ik_a r(x_a)} \ , \qquad \sum_{a=1}^{N} k_a \ = \ 0 \ . \tag{3.7}$$

An example is given at the end of subsection 3.3.

Let us now analyze the theory by power-counting. We use internal units $\mu \sim 1/x$, and note $[x]_x = 1$, and $[\mu]_x = -[\mu]_\mu = -1$. The dimension of the field and of the coupling-constant are:

$$\nu := [r]_x = \frac{2-D}{2} \ , \quad \varepsilon := [b\mu^\varepsilon]_\mu = 2D - \nu d \ . \tag{3.8}$$

In the sense of Wilson [2] the interaction is relevant for $\varepsilon > 0$, see figure 3.1. Perturbation theory is then expected to be UV-finite except for subtractions associated to relevant operators. We shall come back to this point later.

For clarity, we represent graphically the different interaction terms which have to be considered. The local operators are

$$1 = \mathbf{1} \tag{3.9}$$

$$\frac{1}{2}(\nabla r(x))^2 = \ \text{} \ . \tag{3.10}$$

The bi-local operator, the dipole, is

$$\tilde{\delta}^d(r(x) - r(y)) = \ \text{ 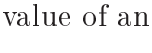 } \ . \tag{3.11}$$

The expectation-value of an observable is

$$\langle \mathcal{O}[r] \rangle_b = \frac{\int \mathcal{D}[r]\, \mathcal{O}[r]\, \mathrm{e}^{-\mathcal{H}[r]}}{\int \mathcal{D}[r]\, \mathrm{e}^{-\mathcal{H}[r]}} \ . \tag{3.12}$$

Perturbatively, all expectation-values are taken with respect to the free theory:

$$\langle \mathcal{O}[r] \rangle_0 = \frac{\int \mathcal{D}[r]\, \mathcal{O}[r]\, \mathrm{e}^{-\frac{1}{2-D}\int_x \frac{1}{2}(\nabla r(x))^2}}{\int \mathcal{D}[r]\, \mathrm{e}^{-\frac{1}{2-D}\int_x \frac{1}{2}(\nabla r(x))^2}} \ . \tag{3.13}$$

A typical term in the expansion of (3.12) is

$$(-bZ_b\mu^\varepsilon)^n \iint \ldots \iint \langle \mathcal{O} \ \text{ 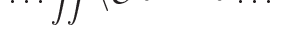 } \ \ldots \ \text{} \rangle_0^{\mathrm{c}} \ , \tag{3.14}$$

where the integral runs over the positions of all dipole-endpoints.

3.2 Locality of divergences

In this section, we show that all divergences are short distance divergences. Note that even for massless theories and in the absence of IR-divergences, this is not trivial. Divergences could as well appear, when some of the distances involved become equal, or multiple of each other. A simple counter-example is the integral of $\Big||a|-|b|\Big|^{-\nu d}$, where a and b are two of the distances involved.

That divergences only occur at short distances (i.e. when at least one of the distances involved tends to 0), is a consequence of Schoenbergs theorem [145]. Here, we present an proof, based on the equivalence with electrostatics.

We first state that with our choice of normalizations (see appendix A.1), the free correlation-function $C(x_1,x_2)$

$$\begin{aligned} C(x_1,x_2) := \frac{1}{d}\left\langle \frac{1}{2}\left[r(x_1)-r(x_2)\right]^2\right\rangle_0 &= |x_1-x_2|^{2-D} \\ &\equiv (2-D)S_D\int\frac{\mathrm{d}^Dp}{(2\pi)^D}\,\frac{1}{p^2}\left(1-\mathrm{e}^{ip(x_1-x_2)}\right) \end{aligned} \tag{3.15}$$

is the Coulomb potential in D dimensions. Furthermore, the interaction part of the Hamiltonian $\mathcal{H}$ is reminiscent of a dipole, and can be written as

$$\begin{aligned} \mathcal{H}_{\mathrm{int}} &= bZ_b\mu^\varepsilon\int_{x_1}\int_{x_2}\tilde{\delta}^d(r(x_1)-r(x_2)) \\ &= bZ_b\mu^\varepsilon\int_{x_1}\int_{x_2}\int_k \mathrm{e}^{ik[r(x_1)-r(x_2)]}\ , \end{aligned} \tag{3.16}$$

where k may be seen as a d-component (vector-) charge.

The next step is to analyze the divergences appearing in the perturbative calculation of expectation values of observables. To simplify the calculations, we focus on the normalized partition function

$$\frac{\mathcal{Z}}{\mathcal{Z}_0} = \frac{1}{\mathcal{Z}_0}\sum_{\text{all configurations}}\mathrm{e}^{-\mathcal{H}} = \left\langle \mathrm{e}^{-\mathcal{H}_{\mathrm{int}}}\right\rangle_0\ . \tag{3.17}$$

To exhibit the similarity to Coulomb systems, consider the second order term

$$\begin{aligned} \frac{1}{2}\left\langle\mathcal{H}_{\mathrm{int}}^2\right\rangle_0 &= \frac{\left(bZ_b\mu^\varepsilon\right)^2}{2}\int_{x_1}\int_{x_2}\int_{y_1}\int_{y_2}\int_k\int_p\left\langle \mathrm{e}^{ik[r(x_1)-r(x_2)]}\,\mathrm{e}^{ip[r(y_1)-r(y_2)]}\right\rangle_0 \\ &= \frac{\left(bZ_b\mu^\varepsilon\right)^2}{2}\int_{x_1}\int_{x_2}\int_{y_1}\int_{y_2}\int_k\int_p \mathrm{e}^{-E_{\mathrm{c}}} \\ E_{\mathrm{c}} &= k^2C(x_1-x_2)+p^2C(y_1-y_2) \\ &\quad +kp\left[C(x_1-y_2)+C(x_2-y_1)-C(x_1-y_1)-C(x_2-y_2)\right]\ , \end{aligned} \tag{3.18}$$

where E_{c} is the Coulomb-energy of a configuration of dipoles with charges $\pm k$, and $\pm p$, respectively. More generally, for any number of dipoles (and even for any Gaussian measure) we have

$$\left\langle \mathrm{e}^{i\sum_i k_i r(x_i)}\right\rangle_0 = \mathrm{e}^{-E_{\mathrm{c}}}\ , \qquad E_{\mathrm{c}} = \frac{1}{2}\sum_{i,j}\left\langle k_i r(x_i)\, k_j r(x_j)\right\rangle_0\ . \tag{3.19}$$

Since $\sum_i k_i = 0$, the latter can be rewritten with the help of the usual correlation function $C(x-y) = \frac{1}{2d}\left\langle [r(x)-r(y)]^2 \right\rangle_0$ as

$$E_{\rm c} = -\frac{1}{4d} \sum_{i,j} k_i k_j \left\langle [r(x_i)-r(x_j)]^2 \right\rangle_0 \ . \tag{3.20}$$

As for any configuration of dipoles, specified by their coordinates and charges, the total charge is zero, the Coulomb-energy is bounded from below, i.e.

$$E_{\rm c} \geq 0 \ . \tag{3.21}$$

Formally, this is proven by the following line of equalities (remember that $D < 2$)

$$\begin{aligned} E_{\rm c} &= \frac{1}{2} \sum_{i,j} \langle k_i r(x_i)\, k_j r(x_j) \rangle_0 \\ &= \frac{(2-D)S_D}{2} \int \frac{{\rm d}^D p}{(2\pi)^D} \sum_{i,j} k_i k_j \frac{1}{p^2} {\rm e}^{ip(x_i - x_j)} \\ &= \frac{(2-D)S_D}{2} \int \frac{{\rm d}^D p}{(2\pi)^D} \frac{1}{p^2} \left| \sum_i k_i {\rm e}^{ipx_i} \right|^2 \geq 0 \ . \end{aligned} \tag{3.22}$$

The last inequality is again due to the global charge neutrality, which ensures convergence of the integral for small p. Hence, $E_{\rm c}$ vanishes, if and only if the charge density vanishes everywhere. This implies that

$${\rm e}^{-E_{\rm c}} \leq 1 \ , \tag{3.23}$$

and the equality is obtained for vanishing charge density. Noting $E_{\rm c} = \sum_{i,j} k_i k_j Q_{ij}$, Eq. (3.22) even states that as long as $x_i \neq x_j$ for all $i \neq j$, Q_{ij} is a non-degenerate form on the space of k_i with $\sum_i k_i = 0$. This implies that integrating ${\rm e}^{-E_{\rm c}}$ as in Eq. (3.18) over all k_i with $\sum_i k_i = 0$ gives a finite result, as long as not some of the x_i coalesce. Consequently, divergences in the integration over x_i can only appear when at least some of the distances vanish, as stated above.

This does of course not rule out IR-divergences. We will see later that they are absent in translationally invariant observables. An explicit example is given at the end of the next section; for a proof see [57].

3.3 More about perturbation theory

Let us apply the above observation to evaluating the integrals in Eq. (3.18); this will give an intuitive idea of the kind of counter-terms needed to cancel the UV-divergences, as will be made formal later. The basic idea is to look for classes of configurations which are similar. The integral over the parameter which indexes such configurations is the product of a divergent factor, and a "representative" operator. For the case of two dipoles, one with charge k and the other with charge $p-k$, and approaching its endpoints (as indicated by the dashed lines below), one only sees a single dipole with charge p from far away, i.e.

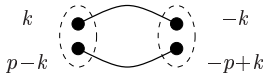

$$\approx \ p \bullet\!\!-\!\!-\!\!\bullet -p \ \times \ {\rm e}^{-k^2(|s|^{2-D}+|t|^{2-D})} \ . \tag{3.24}$$

The second factor on the r.h.s. contains the dominant part of the Coulomb energy $E_c = k^2(|s|^{2-D} + |t|^{2-D})$ of the interaction between the two dipoles; s and t are the distances between the contracted (approached) ends. The integral over k is now factorized, and we obtain

$$\int_k \mathrm{e}^{-k^2(|s|^{2-D}+|t|^{2-D})} = (|s|^{2-D} + |t|^{2-D})^{-d/2} \ . \tag{3.25}$$

Finally integrating over p in Eq. (3.24) gives back the δ-interaction •—— multiplied with (), where we define the coefficient as

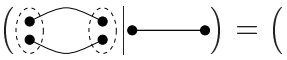

$$= \left(|s|^{2-D} + |t|^{2-D}\right)^{-d/2} \ . \tag{3.26}$$

The notation, which will be explained later, reminds of a scalar product or projection of a singular configuration of two dipoles onto a single dipole. Eq. (3.26) contains the dominant UV-divergence upon approaching the endpoints; this will be made formal later.

As an example of an expectation value, use in Eq. (3.7) the observable $\mathcal{O} = \mathrm{e}^{ik[r(s)-r(t)]}$, which is the generating function for the moments of $[r(s) - r(t)]$; the series up to first order in b reads (remind $Z_b = 1 + O(b)$)

$$\begin{aligned}\langle\mathcal{O}\rangle_b = \mathrm{e}^{-k^2C(s-t)} \times \\ \left\{1 + b\mu^\varepsilon \int_x \int_y \left[1 - \exp\left(\frac{1}{4}k^2 \frac{[C(s-x)+C(t-y)-C(s-y)-C(t-x)]^2}{C(x-y)}\right)\right] C(x-y)^{-d/2}\right. \\ \left. + O(b^2)\right\} \ .\end{aligned} \tag{3.27}$$

Note that the integral over x and y is IR-convergent, but UV-divergent at $\varepsilon \leq 0$: There is a singularity for $|x - y| \to 0$. This is a general feature of such expectation values. The purpose of the rest of this section is to introduce the basic tools to handle these divergences. On the example of Eq. (3.27), this is verified in exercise 6, see page 178.

3.4 Operator product expansion (OPE), a pedagogical example

Throughout this review, we will use the techniques of normal-ordering and operator product expansion to analyze the short distance behavior of the theory. Since their technical simplicity is as little recognized as their 1 to 1 correspondence to standard Feynman-graphs, we shall give here a pedagogical derivation of the 2-loop result for the exponent η in standard scalar ϕ^4 theory, before discussing the case of a membrane in the next section. Complementary material can be found in [146]. Readers familiar with the procedure can continue with section 3.5.

Define the renormalized ϕ^4-Hamiltonian as

$$\mathcal{H} = \frac{Z}{d-2} \int_x \frac{1}{2}(\nabla\phi(x))^2 + bZ_b\mu^\epsilon \int_x :\phi^4(x): \ . \tag{3.28}$$

The integration measure is normalized as

$$\int_x = \frac{1}{S_d} \int \mathrm{d}^d x \ , \qquad S_d = 2\frac{\pi^{d/2}}{\Gamma(d/2)} \ , \tag{3.29}$$

where S_d is the surface of the d-dimensional unit sphere. This is done in order to obtain for the free expectation values (denoted by subscript $_0$)

$$C(x-y) := \langle \phi(x)\phi(y) \rangle_0 = |x-y|^{2-d} \ . \tag{3.30}$$

Note the similarity and difference between the definitions in Eq. (3.15) and Eq. (3.30); the difference results from the 0-mode, which has to be subtracted in the case of polymers and membranes ($D < 2$), but not of the ϕ^4-model ($d > 2$).

The dimensional regularization parameter ϵ is

$$\epsilon = 4 - d \ , \tag{3.31}$$

and μ is the renormalization (subtraction) scale. Note the difference to Eq. (3.8), where we use ε instead of ϵ. The renormalization Z-factors, introduced to render the theory finite, start with 1, and higher order terms in b will be added to cancel the divergences.

The dots ":" indicate the normal-order procedure. We define the normal order of an operator $\mathcal{O}$ as

$$:\mathcal{O}: \ = \mathcal{O} - \text{all tadpole-like diagrams constructed from } \mathcal{O} \ . \tag{3.32}$$

In other words: By normal-ordering an operator, we just subtract all self-contractions. Let us give some examples

$$\begin{aligned} :\phi^2(x): \ &= \ \phi^2(x) - C(0) \ \mathbf{1} \\ :\phi^4(x): \ &= \phi^4(x) - 6C(0) \ :\phi^2(x): \ -3C^2(0) \ \mathbf{1} \end{aligned} \tag{3.33}$$

Note that on the right-hand side all subtracted terms are normal-ordered. One can of course recursively replace them, which for $:\phi^4(x):$ e.g. leads to

$$:\phi^4(x): = \phi^4(x) - 6C(0)\phi^2(x) + 3C^2(0) \ \mathbf{1} \ . \tag{3.34}$$

In the dimensional regularization scheme, these relations are much simplified through the rule that $C(0) \equiv 0$. Note also that the normal-order prescription is associative.

Normal ordering is a powerful tool to organize the perturbation expansion. Let us show this by proceeding to the real calculation. We want to study the short-distance behavior of two operators $:\phi^4(x):$ and $:\phi^4(y):$ in an OPE. To this aim we first normal-order the product of the two interactions:

$$\begin{aligned} :\phi^4(x)::\phi^4(y): = \ & :\phi^4(x)\phi^4(y): \\ & +16 \ :\phi^3(x)\phi^3(y): \, C(x-y) \\ & +72 \ :\phi^2(x)\phi^2(y): \, C^2(x-y) \\ & +96 \ :\phi(x)\phi(y): \, C^3(x-y) \\ & +24 \ \ \mathbf{1} \ C^4(x-y) \ . \end{aligned} \tag{3.35}$$

It is now essential that the normal-ordered product of two operators is free of divergences when these operators are approached; the divergences are contained in the factors of powers of $C(x-y)$. E.g. at leading order, the first term in Eq. (3.35) becomes

$$:\phi^4(x)\phi^4(y): = :\phi^8(z): + \dots \ , \tag{3.36}$$

where $z = \frac{x+y}{2}$. Let us now consider the perturbation expansion of the expectation value of an observable $\mathcal{O}$

$$\langle \mathcal{O} \rangle_b := \frac{1}{Z} \int \mathcal{D}[\phi] \, \mathrm{e}^{-\mathcal{H}} \, \mathcal{O} = \left\langle \mathrm{e}^{-bZ_b \mu^\epsilon \int :\phi^4(x):} \, \mathcal{O} \right\rangle_0^{\mathrm{conn}} \quad , \tag{3.37}$$

where $\langle \ldots \rangle_0$ denotes the free expectation value, and we retain only diagrams that are connected to points in the observable $\mathcal{O}$. The term quadratic in b contains (setting all Z-factors equal to 1 for the moment)

$$\frac{b^2 \mu^{2\epsilon}}{2} \int_x \int_y :\phi^4(x): :\phi^4(y): \, \mathcal{O} \ , \tag{3.38}$$

Observe now that

$$\int_x \int_y :\phi^4(x): :\phi^4(y): \tag{3.39}$$

possesses short-distance divergences according to Eq. (3.35). More explicitly, the first two terms, $:\phi^4(x)\phi^4(y):$ and $16 \, :\phi^3(x)\phi^3(y): C(x-y)$ are free of divergences when $|x-y| \to 0$. The third one is upon integration over x and y

$$72 \int_x \int_y :\phi^2(x)\phi^2(y): C^2(x-y) = 72 \, A \int_z :\phi^4(z): + \text{finite} \ , \tag{3.40}$$

where

$$A = \int_t C^2(t) = \int_0^{\mu^{-1}} \frac{\mathrm{d}t}{t} t^d \times t^{2(2-d)} = \frac{1}{\epsilon} \mu^{-\epsilon} \ . \tag{3.41}$$

It is very important to note that the integral over $C^2(x-y)$ is localized at $x - y = 0$. This means that for any smooth function $f(x,y)$

$$\int_x \int_y C^2(x-y) \, f(x,y) = \frac{\mu^{-\epsilon}}{\epsilon} \int_z f(z,z) + O(\epsilon^0) \ , \tag{3.42}$$

or more formally that $C^2(x-y)$ becomes in the limit of $\epsilon \to 0$ a distribution

$$C^2(x-y) = \frac{\mu^{-\epsilon}}{\epsilon} S_d \delta^d(x-y) + O(\epsilon^0) \ . \tag{3.43}$$

This explains why in Eq. (3.40) we could simply replace $:\phi^2(x)\phi^2(y):$ by $:\phi^4(z):$. It is now easy to see that after introduction of a renormalization factor

$$Z_b = 1 + 36 \frac{b}{\epsilon} \tag{3.44}$$

a second term of order b^2 will appear in the perturbation expansion, namely

$$-36 \frac{b^2 \mu^\epsilon}{\epsilon} \int_z :\phi^4(z): \, \mathcal{O} \ , \tag{3.45}$$

which will cancel the divergence. This is the only renormalization necessary at 1-loop order. Especially, no counter-term for $\int_x \frac{1}{2} :(\nabla\phi(x))^2:$ is necessary at leading order in b. However, it demands a renormalization at second order, arising form the term

$$:\phi(x)\phi(y): C^3(x-y) \ . \tag{3.46}$$

As above, we now have to analyze the integral ($t = x - y$)

$$\int\limits_t C^3(t) \, :\phi(x)\phi(y): \ . \tag{3.47}$$

Noting that

$$\int\limits_t C^3(t) = \int \frac{\mathrm{d}t}{t} t^d \, t^{3(2-d)} = \int \frac{\mathrm{d}t}{t} t^{2\epsilon-2} \tag{3.48}$$

the leading term is a relevant (quadratic) divergence. We therefore have to expand $\phi(x)$ and $\phi(y)$ up to second order

$$\phi(x) = \phi(z) + \frac{x-y}{2} \nabla\phi(z) + \frac{1}{2} \left(\frac{y-x}{2} \nabla \right)^2 \phi(z) + O\left((x-y)^3 \right) \tag{3.49}$$

to obtain

$$\begin{aligned} :\phi(x)\phi(y): \ &= \ :\left[\phi(z) + \frac{x-y}{2} \nabla\phi(z) + \frac{1}{2} \left(\frac{x-y}{2} \nabla \right)^2 \phi(z) + O\left((x-y)^3 \right) \right] \times \\ &\qquad \left[\phi(z) + \frac{y-x}{2} \nabla\phi(z) + \frac{1}{2} \left(\frac{y-x}{2} \nabla \right)^2 \phi(z) + O\left((x-y)^3 \right) \right] : \\ &= :\phi(z)^2: - \frac{1}{4} :[(x-y)\nabla\phi(z)]^2: + \frac{1}{4} :\phi(z) \left[(x-y)\nabla \right]^2 \phi(z): + O\left((x-y)^3 \right) \ . \end{aligned} \tag{3.50}$$

With the help of Eq. (3.48), Eq. (3.47) becomes

$$\begin{aligned} &\int\limits_0^{\mu^{-1}} \frac{\mathrm{d}t}{t} t^{2\epsilon-2} \left[:\phi(z)^2: - \frac{t^2}{4d} :(\nabla\phi(z))^2: + \frac{t^2}{4d} :\phi(z)\Delta\phi(z): + O\left((t)^3 \right) \right] \\ &\qquad = \frac{\mu^{2-2\epsilon}}{-2+2\epsilon} :\phi(z)^2: \ - \frac{\mu^{-2\epsilon}}{2\epsilon} \frac{1}{4d} \left[:(\nabla\phi(z))^2: - :\phi(z)\Delta\phi(z): \right] + \text{finite} \ . \end{aligned} \tag{3.51}$$

The first term does not come with a pole in $1/\epsilon$ and in addition scales to 0 in the large $L = 1/\mu$ limit. It will thus be neglected. The remaining two terms are equivalent up to a total derivative, and thus Eq. (3.38) yields another divergent term

$$\frac{24 b^2}{d\epsilon} \int\limits_z \frac{1}{2} :(\nabla\phi(z))^2: \ \mathcal{O} \ . \tag{3.52}$$

This is renormalized (canceled) by setting

$$Z = 1 - \frac{24(d-2)}{d} \frac{b^2}{\epsilon} = 1 - 12 \frac{b^2}{\epsilon} + \text{finite} \ . \tag{3.53}$$

The last step is as usual to calculate the renormalization group functions $\beta(b)$ and $\eta(b)$, quantifying the flow of the coupling b and the field ϕ upon changing μ [147][1]. The result is

$$\beta(b) := \mu \frac{\partial}{\partial \mu}\bigg|_0 b = -\epsilon b + 36 b^2 + O(b^3) \tag{3.54}$$

$$\eta(b) := \mu \frac{\partial}{\partial \mu}\bigg|_0 \ln Z = 24 b^2 + O(b^3) \ . \tag{3.55}$$

Note that the β-function has a non-trivial IR-stable fixed point ($\beta(b^*) = 0$) at $b^* = \epsilon/36$ and that this is sufficient to get the exponent η up to order ϵ^2:

$$\eta = \eta(b^*) = \frac{\epsilon^2}{54} \ . \tag{3.56}$$

Finally, let us still note the equivalence of the OPE with standard Feynman-diagrams. The first integral was

$$:\phi^2(x)\phi^2(y): \int\limits_{x-y} C^2(x-y) = \tag{3.57}$$

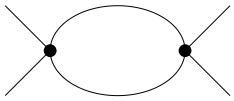

Usually, this is written in momentum space as

$\xrightarrow{p}$

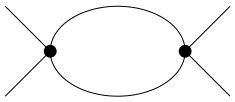

$$= \int\limits_k \frac{1}{(k+p)^2}\frac{1}{k^2} \ . \tag{3.58}$$

The other diagram was

$$:\phi(x)\phi(y): \int\limits_{x-y} C^3(x-y) = \tag{3.59}$$

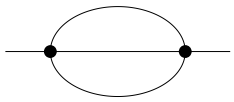

Note that if we parameterize the latter by the momentum p which is running through, then

$\xrightarrow{p}$

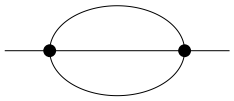

$$= \int\limits_{q_1}\int\limits_{q_2} \frac{1}{q_1^2}\frac{1}{q_2^2}\frac{1}{(q_1+q_2+p)^2} \sim \frac{1}{\epsilon} p^{2-2\epsilon} \ . \tag{3.60}$$

The factor of p^2 is the equivalent of the derivatives appearing in Eq. (3.51).

3.5 Multilocal operator product expansion (MOPE)

In section 3.2, we showed that for self-avoiding membranes divergences only occur at short distances. The situation is thus similar to local field-theories for which we discussed in the last section how the techniques of operator product expansion can be used to analyze the divergences. Our aim is now, to generalize these techniques to the multilocal case [56,57]. Intuitively, in the context of multilocal theories – by which we mean that the interaction

[1] For membranes, a derivation of the renormalization group functions is given in appendix A.4

depends on more than one point – we also expect multilocal operators to appear in such an operator product expansion, which therefore will be called "multi-local operator product expansion" (MOPE). Its precise definition is the aim of this section, whereas we shall calculate some examples in the following one.

We start our analysis by recalling the general form of a (local) operator product expansion of two scaling-operators $\Phi_A(z+\lambda x)$ and $\Phi_B(z+\lambda y)$ in a massless theory in the limit of $\lambda \to 0$:

$$\Phi_A(z+\lambda x)\Phi_B(z+\lambda y) = \sum_i C_i(z,\lambda x,\lambda y)\,\Phi_i(z)\ , \tag{3.61}$$

where $C_i(z,\lambda x,\lambda y)$ are homogeneous functions of λ

$$C_i(z,\lambda x,\lambda y) = \lambda^{[\Phi_A]_x+[\Phi_B]_x-[\Phi_i]_x} C_i(z,x,y)\ . \tag{3.62}$$

Here $[\Phi]_x$ is the canonical dimension of the operator Φ in space-units such that $[x]_x = 1$, as obtained by naive power-counting. If the theory is translationally invariant, $C_i(z,x,y)$ is also independent of z, and we will suppose that this is the case, if not stated otherwise[2]. Also recall that this relation is to be understood as an operator identity, i.e. it holds inserted into *any* expectation value, as long as none of the other operators sits at the point z, to which the contraction is performed.

An example for the multilocal theory is

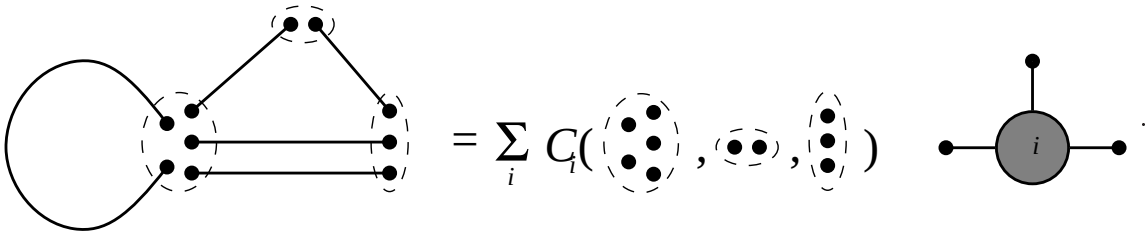

(3.63)

Let us explain the formula. We consider n dipoles (here $n=5$) and we separate the $2n$ end-points into m subsets (here $m=3$) delimited by the dashed lines. The MOPE describes how the product of these n dipoles behaves when the points inside each of the m subsets are contracted towards a single point z_j. The result is a sum over *multilocal* operators $\Phi_i(z_1,\ldots,z_m)$, depending on the m points $z_1,\ldots,z_m$, of the form

$$\sum_i C_i(x_1-z_1,\ldots)\,\Phi_i\left(z_1,z_2,\ldots,z_m\right)\ , \tag{3.64}$$

where the MOPE-coefficients $C_i(x_1-z_1,\ldots)$ depend only on the distances $x_l - z_j$ *inside each subset*. This expansion is again valid as an operator-identity, i.e. inserted into any expectation value and in the limit of small distances between contracted points. Again, no other operator should appear at the points $z_1,\ldots,z_m$, towards which the operators are contracted. As the Hamiltonian (3.1) does not contain a mass-scale, the MOPE-coefficients are as in Eq. (3.62) homogeneous functions of the relative positions between the

[2]Translation invariance is e.g. broken when regarding systems with boundaries or initial time problems, see section 8.4 and [148] for a review. It is also broken when the underlying metric is not constant, see [57,149].

contracted points, with the degree of homogeneity given by simple dimensional analysis. In the case considered here, where n dipoles are contracted to an operator Φ_i, this degree is simply $-n\nu d - [\Phi_i]_x$. This means that

$$C_i(\lambda(x_1 - z_1), \ldots) = \lambda^{-n\frac{2-D}{2}d - [\Phi_i]_x} C_i(x_1 - z_1, \ldots) \ , \tag{3.65}$$

where $[\Phi_i]_x$ is the canonical dimension of the operator Φ_i and $-d(2-D)/2$ is simply the canonical dimension of the dipole.

In order to evaluate the associated singularity, one finally has to integrate over all relative distances inside each subset. This gives an additional scale factor with degree $D(2n-m)$. A singular configuration, such as in Eq. (3.63), will be UV-divergent if this degree of divergence

$$D(2n-m) - n\frac{2-D}{2}d - [\Phi_i]_x \ , \tag{3.66}$$

is negative. It is superficially divergent if the degree is zero and convergent otherwise. The idea of renormalization, formalized in section 3.8 and proven to work in section 5, is *to remove exactly these superficially divergent contributions recursively.*

3.6 Evaluation of the MOPE-coefficients

The MOPE therefore gives a convenient and powerful tool to calculate the dominant and all subdominant contributions from singular configurations. In this section, we explain how to calculate the MOPE-coefficients on some explicit examples. These examples will turn out to be the necessary diagrams at 1-loop order.

In the following we shall use the notion of normal-ordering introduced in section 3.4. The first thing, which we use, is that

$$:\mathrm{e}^{ikr(x)}: = \mathrm{e}^{ikr(x)} \ . \tag{3.67}$$

Explicitly, tadpole-like contributions which are powers of

$$\int \mathrm{d}^D p \, \frac{1}{p^2} \tag{3.68}$$

are omitted. This is done via a finite part prescription (analytic continuation, dimensional regularization), valid for infinite membranes, for which the normal-order prescription is defined. Let us stress that this is a pure technical trick, which is not really necessary. However, adopting this notation, the derivation of the MOPE-coefficients is much simplified, and we will henceforth stick to this convention. The suspicious reader may always check that the same results are obtained without this procedure. This is clear from the uniqueness of the finite-part prescription.

The key-formula for all further manipulations is

$$:\mathrm{e}^{ikr(x)}::\mathrm{e}^{ipr(y)}: = \ \mathrm{e}^{kpC(x-y)} \ :\mathrm{e}^{ikr(x)}\mathrm{e}^{ipr(y)}: \ . \tag{3.69}$$

This can be proven as follows: Consider the (free) expectation value of any observable $\mathcal{O}$ times the operators of Eq. (3.69). Then the the left- and right-hand sides of the above

equation read

$$\mathcal{L} = \left\langle \mathcal{O} :\mathrm{e}^{ikr(x)}::\mathrm{e}^{ipr(y)}: \right\rangle_0$$
$$\mathcal{R} = \mathrm{e}^{kpC(x-y)} \left\langle \mathcal{O} :\mathrm{e}^{ikr(x)}\mathrm{e}^{ipr(y)}:\right\rangle_0 \ .$$

First of all, for $\mathcal{O} = 1$, the desired equality of $\mathcal{L} = \mathcal{R}$ holds, because $\left\langle :\mathrm{e}^{ikr(x)}\mathrm{e}^{ipr(y)}:\right\rangle_0 = 1$ and $\left\langle :\mathrm{e}^{ikr(x)}::\mathrm{e}^{ipr(y)}:\right\rangle_0 = \mathrm{e}^{kpC(x-y)}$. Now consider a non-trivial observable $\mathcal{O}$, and contract all its fields r with $\mathrm{e}^{ikr(x)}$ or $\mathrm{e}^{ipr(y)}$, before contracting any of the fields $r(x)$ with $r(y)$. The result is a product of correlation-functions between the points in $\mathcal{O}$ and x or y, and these are equivalent for both $\mathcal{L}$ and $\mathcal{R}$. However, contracting an arbitrary number of times $\mathrm{e}^{ikr(x)}$, leaves the exponential $\mathrm{e}^{ikr(x)}$ invariant. Completing the contractions for $\mathcal{L}$ therefore yields a factor of $\mathrm{e}^{kpC(x-y)}$, and the latter one also appears in $\mathcal{R}$. Thus, the equality of $\mathcal{L}$ and $\mathcal{R}$ holds for all $\mathcal{O}$ and this proves Eq. (3.69).

Now proceed to the first explicit example, the contraction of a single dipole with endpoints x and y.

$$= \int_k :\mathrm{e}^{ikr(x)}::\mathrm{e}^{-ikr(y)}: \ . \tag{3.70}$$

This configuration may have divergences when x and y come close together. Let us stress that in contrast to ϕ^4-theory, these divergences are not obtained as a finite sum of products of correlators: Since $C(x-y) = |x-y|^{2-D}$, the latter is always well-behaved at $x = y$. The singularity only appears when summing an infinite series of diagrams as we will do now. To this purpose, we first normal-order the two exponentials using Eq. (3.69)

$$\int_k :\mathrm{e}^{ik[r(x)-r(y)]}: \mathrm{e}^{-k^2|x-y|^{2\nu}} \ . \tag{3.71}$$

Note that the operators $\mathrm{e}^{ikr(x)}$ and $\mathrm{e}^{-ikr(y)}$ are free of divergences upon approaching each other, since no more contractions can be made. The divergence is captured in the factor $\mathrm{e}^{-k^2|x-y|^{2\nu}}$. Therefore, we can expand the exponential $:\mathrm{e}^{ik[r(x)-r(y)]}:$ for small $x-y$ and consequently in powers of $[r(x)-r(y)]$. This expansion is

$$\int_k :\left\{\mathbf{1} + ik\left[r(x)-r(y)\right] - \frac{1}{2}\left(k\left[r(x)-r(y)\right]\right)^2 + \ldots\right\}: \mathrm{e}^{-k^2|x-y|^{2\nu}} \ . \tag{3.72}$$

We truncated the expansion after the third term. It will turn out later that this is sufficient, since subsequent terms in the expansion are proportional to irrelevant operators for which the integral over the MOPE-coefficient is UV-convergent.

Due to the symmetry of the integration over k the term linear in k vanishes. Also due to symmetry, the next term can be simplified with the result

$$\int_k \left[\mathbf{1} - \frac{k^2}{2d} \ :\left[r(x)-r(y)\right]^2: + \ldots\right] \mathrm{e}^{-k^2|x-y|^{2\nu}} \ . \tag{3.73}$$

Finally, the integration over k can be performed. Recall that normalizations were chosen such that $\int_k \mathrm{e}^{-sk^2} = s^{-d/2}$ to obtain

$$|x-y|^{-\nu d}\,\mathbf{1} - \frac{1}{4} \ :\left[(x-y)\nabla r\left(\frac{x+y}{2}\right)\right]^2: \ |x-y|^{-\nu(d+2)} + \ldots \ . \tag{3.74}$$

The second operator has a tensorial structure, which has to be taken into account in order to construct the subtraction operator. Using the short-hand notation ${}_\alpha\!\!\bullet\!\!-\!\!\bullet_\beta = \frac{1}{2}(\partial_\alpha r)(\partial_\beta r)$, we can write this symbolically as

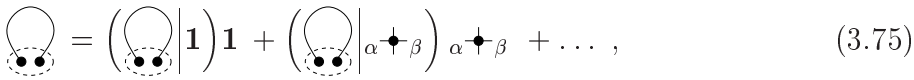

$$= \left(\quad\middle|\mathbf{1}\right)\mathbf{1} + \left(\quad\middle|{}_\alpha\!\!\bullet\!\!-\!\!\bullet_\beta\right){}_\alpha\!\!\bullet\!\!-\!\!\bullet_\beta + \dots \,, \tag{3.75}$$

with the MOPE-coefficients (reminding Feynman's bra-ket notation)

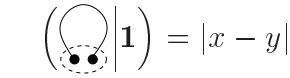

$$= |x-y|^{-\nu d} \tag{3.76}$$

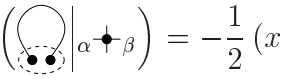

$$= -\frac{1}{2}\,(x-y)_\alpha\,(x-y)_\beta\,|x-y|^{-\nu(d+2)}\,. \tag{3.77}$$

As long as the angular average is taken (and this will be the case when integrating the MOPE-coefficient to obtain the divergence), we can replace in Eq. (3.75) ${}_\alpha\!\!\bullet\!\!-\!\!\bullet_\beta$ by $\bullet\!\!-\!\!\bullet := \frac{1}{2}(\nabla r)^2$ and Eq. (3.77) by

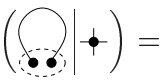

$$= -\frac{1}{2D}|x-y|^{D-\nu d}\,. \tag{3.78}$$

Next consider a real multi-local example of an operator-product expansion, namely the contraction of two dipoles towards a single dipole:

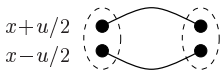

$$= \int\limits_k \mathrm{e}^{ik[r(x+u/2)-r(y+v/2)]} \int\limits_p \mathrm{e}^{ip[r(x-u/2)-r(y-v/2)]}\,. \tag{3.79}$$

This has to be analyzed for small u and v, in order to control the divergences in the latter distances. As above, we normal-order operators which are approached, yielding

$$\mathrm{e}^{ikr(x+u/2)}\mathrm{e}^{ipr(x-u/2)} = :\mathrm{e}^{ikr(x+u/2)}::\mathrm{e}^{ipr(x-u/2)}: = :\mathrm{e}^{ikr(x+u/2)}\mathrm{e}^{ipr(x-u/2)}:\,\mathrm{e}^{kpC(u)}\,. \tag{3.80}$$

A similar formula holds when approaching $\mathrm{e}^{-ikr(y+v/2)}$ and $\mathrm{e}^{-ipr(y-v/2)}$

$$\mathrm{e}^{-ikr(y+v/2)}\mathrm{e}^{-ipr(y-v/2)} = :\mathrm{e}^{-ikr(y+v/2)}::\mathrm{e}^{-ipr(y-v/2)}: = :\mathrm{e}^{-ikr(y+v/2)}\mathrm{e}^{-ipr(y-v/2)}:\,\mathrm{e}^{kpC(v)}\,. \tag{3.81}$$

Eq. (3.79) then becomes

$$\int\limits_k \int\limits_p :\mathrm{e}^{ikr(x+u/2)+ipr(x-u/2)}:\,:\mathrm{e}^{-ikr(y+v/2)-ipr(y-v/2)}:\,\mathrm{e}^{kp[C(u)+C(v)]}\,. \tag{3.82}$$

In order to keep things as simple as possible, let us first extract the leading contribution before analyzing subleading corrections. This leading contribution is obtained when expanding the exponential operators (here exemplified for the second one) as

$$:\mathrm{e}^{-ikr(y+v/2)}\mathrm{e}^{-ipr(y-v/2)}: = :\mathrm{e}^{-i(k+p)r(y)}\,(1+O(\nabla r)): \tag{3.83}$$

and dropping terms of order ∇r. This simplifies Eq. (3.82) to

$$\int\limits_k \int\limits_p :\mathrm{e}^{i(k+p)r(x)}:\,:\mathrm{e}^{-i(k+p)r(y)}:\,\mathrm{e}^{kp[C(u)+C(v)]}\,. \tag{3.84}$$

In the next step, first k and second p are shifted

$$k \longrightarrow k - p \ , \quad \text{then} \qquad p \longrightarrow p + \frac{k}{2} \ . \tag{3.85}$$

The result is (dropping the normal-ordering according to Eq. (3.67))

$$\int\limits_k \mathrm{e}^{ik[r(x)-r(y)]} \int\limits_p \mathrm{e}^{(\frac{1}{4}k^2-p^2)[C(u)+C(v)]} \ . \tag{3.86}$$

The factor of $\int_k \mathrm{e}^{ik[r(x)-r(y)]}$ is again a δ-distribution, and the leading term of the short distance expansion of Eq. (3.86). Derivatives of the δ-distribution appear when expanding $\mathrm{e}^{(\frac{1}{4}k^2-p^2)[C(u)+C(v)]}$ in k^2; these are less relevant and only the first sub-leading term will be displayed for illustration:

$$\int\limits_k \mathrm{e}^{ik[r(x)-r(y)]} \int\limits_p \mathrm{e}^{-p^2[C(u)+C(v)]} \left(1 + \frac{k^2}{4}\,[C(u)+C(v)] + \ldots\right)$$

$$= \Big($$ 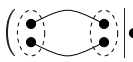 $$\Big)$$ 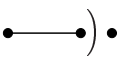 $$+ \Big($$ 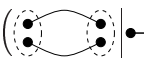 $$\Big)$$ 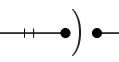 $$+ \ldots \ , \tag{3.87}$$

where in analogy to Eqs. (3.75) and (3.77)

$$\Big($$ 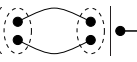 $$\Big) = [C(u)+C(v)]^{-d/2} \ ,$$

$$\Big($$ 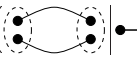 $$\Big) = \frac{1}{4}\,[C(u)+C(v)]^{1-d/2} \tag{3.88}$$

and

$$\text{} = \tilde{\delta}^d(r(x)-r(y)) \ , \qquad \text{} = (-\Delta_r)\tilde{\delta}^d(r(x)-r(y)) \ . \tag{3.89}$$

Let us already mention that the leading contribution proportional to the δ-distribution will renormalize the coupling-constant, and that the next-to-leading term is irrelevant and can be neglected. The same holds true for the additional term proportional to (∇r) which was dropped in Eq. (3.83).

There is one more possible divergent contribution at the 1-loop level, namely  . We now show that the leading term of its expansion, which is expected to be proportional to  , is trivial. To this aim consider

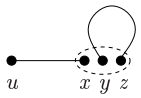

$$= \int\limits_{k,p} :\mathrm{e}^{ikr(u)}: :\mathrm{e}^{-ikr(x)}: :\mathrm{e}^{ipr(y)}: :\mathrm{e}^{-ipr(z)}:$$

$$= \int\limits_{k,p} :\mathrm{e}^{ikr(u)}: :\mathrm{e}^{-ikr(x)}\,\mathrm{e}^{ipr(y)}\,\mathrm{e}^{-ipr(z)}:\ \mathrm{e}^{-p^2C(y-z)}\,\mathrm{e}^{kp[C(x-z)-C(x-y)]} \ . \tag{3.90}$$

We want to study the contraction of x, y, and z, and look for all contributions which are proportional to

$$\text{} = \int\limits_k :\mathrm{e}^{ikr(u)}: :\mathrm{e}^{-ikr((x+y+z)/3)}: \ . \tag{3.91}$$

The key-observation is that in Eq. (3.90) the leading term is obtained by approximating $\mathrm{e}^{kp[C(x-z)-C(x-y)]} \approx 1$. All subsequent terms yield factors of k, which after integration over k give derivatives of the $\tilde{\delta}^d$-distribution. The result is that

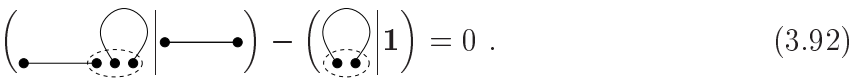

(3.92)

This means that divergences of  are already taken into account by a proper treatment of the divergences in  , analyzed in Eq. (3.75).

3.7 Strategy of renormalization

In the last two sections, we discussed how divergences occur, how their general structure is obtained by the MOPE, and how the MOPE-coefficients are calculated. In the next step, the theory shall be renormalized. The basic idea is to identify the divergences through the MOPE, and then to introduce counter-terms which subtract these divergences. These counter-terms are nothing else than integrals over the MOPE-coefficients, properly regularized, i.e. cut off.

In order to properly understand this point, let us recall the two main strategies employed in renormalization: The first one subtracts divergences in correlation-functions or equivalently vertex-functions. This amounts to adding counter-terms to the Hamiltonian which can be interpreted as a change of the parameters in this Hamiltonian. Calculating observables with this modified Hamiltonian leads to finite physical expectation values, but it is not evident that the integrals appearing in these calculations are convergent.

The other procedure is inspired by ideas employed in a formal proof of renormalizability, or more precisely when applying the **R**-operation to the perturbation expansion, as will be discussed in the next section 5. It consists in adding to the Hamiltonian counter-terms which are *integrals*, such that each *integrand* which appears in the perturbative expansion becomes an integrable function, and *as a consequence* the integrals and thus the perturbation expansion are finite. Of course, to finally obtain the critical exponents, the integral counter-terms have to be reduced to numbers. However, we really want to think of them as integrals in the intermediate steps. The reason is the following: It is extremely difficult to calculate observables. However, this is not really necessary as long as one is only interested in renormalization. The above-mentioned procedure is then sufficient to ensure finiteness of any observable as long as there is no additional divergence when the dipole is contracted towards this observable. The latter situation would require a new counter-term, which is a proper renormalization of the observable itself. The procedure of considering whole integrals as counter-terms is in the heart of our renormalization procedure, and the reader should bear this idea in mind throughout this review.

3.8 Renormalization at 1-loop order

Let us continue on the concrete example of the 1-loop divergences, from which are obtained the scaling exponents to first order in the dimensional regularization parameter ε. Explicitly, the model shall be renormalized through two renormalization group factors Z

(renormalizing the field r) and Z_b (renormalizing the coupling b). Recalling Eq. (3.1), this is

$$\mathcal{H}[r] = \frac{Z}{2-D} \int_x \frac{1}{2} (\nabla r(x))^2 + b Z_b \mu^\varepsilon \int_x \int_y \tilde{\delta}^d (r(x) - r(y)) \ , \tag{3.93}$$

where r and b are the renormalized field and renormalized dimensionless coupling constant, and $\mu = L^{-1}$ is the renormalization momentum scale.

Let us start to eliminate the divergences in the case, where the end-points (x, y) of a single dipole are contracted towards a point (taken here to be the center-of-mass $z = (x+y)/2$). The MOPE is

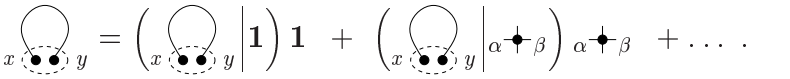

(3.94)

The MOPE-coefficients were obtained in the last section as

$$= |x-y|^{-\nu d} \ , \tag{3.95}$$

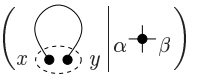

$$= -\frac{1}{2} (x-y)_\alpha (x-y)_\beta |x-y|^{-\nu(d+2)} \ . \tag{3.96}$$

We now have to distinguish between counter-terms for relevant operators and those for marginal operators. The former can be defined by analytic continuation, while the latter require a subtraction scale. Indeed, the divergence proportional to $\mathbf{1}$ is given by the integral

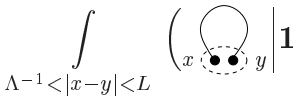

$$= \int_{\Lambda^{-1}}^{L} \frac{\mathrm{d}x}{x} x^{D-\nu d} = \frac{1}{D-\varepsilon} \left(\Lambda^{D-\varepsilon} - L^{\varepsilon - D} \right) \ , \tag{3.97}$$

where Λ is a high-momentum UV-regulator and L a large distance regulator. For $\varepsilon \approx 0$ this is UV-divergent but IR-convergent. The simplest way to subtract this divergence is therefore to replace the dipole operator by

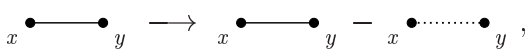

(3.98)

where $x \bullet\cdots\bullet y = |x-y|^{-\nu d}$. This amounts to adding to the bare Hamiltonian (3.1) the UV-divergent counter-term

$$\Delta \mathcal{H}_{\mathbf{1}} = -b Z_b \mu^\varepsilon \int_x \int_y |x-y|^{-\nu d} \ , \tag{3.99}$$

which is a pure number and thus does not change the expectation-value of any physical observable.

We next consider marginal operators: In the MOPE of Eq. (3.94), the integral over the relative distance of $\int_{x-y} \left(x \, y \, \middle| \, \alpha \text{-} \beta \right) \alpha \text{-} \beta$ is logarithmically divergent at $\varepsilon = 0$. In order to find the appropriate counter-term, we use dimensional regularization, i.e. set $\varepsilon > 0$. An

IR-cutoff L, or equivalently a subtraction momentum scale $\mu = L^{-1}$, has to be introduced in order to define the subtraction operation. *As a general rule, let us integrate over all distances appearing in the MOPE-coefficient, bounded by the subtraction scale* $L = \mu^{-1}$. Defining

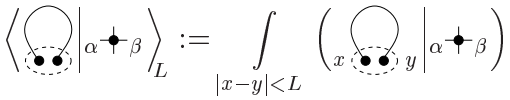

(3.100)

we need the following counter-term in the Hamiltonian

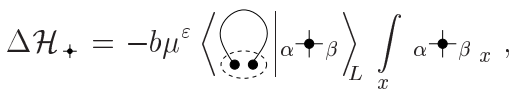

(3.101)

subtracting explicitly the divergence in the integrals, as discussed in the last section. The reader is invited to verify this explicitly in exercise 6 (see page 178) on the example of the expectation value of $\mathcal{O} = \mathrm{e}^{ik[r(s)-r(t)]}$, as given in Eq. (3.27).

Since the angular integration in Eq. (3.100) reduces $_{\alpha}\!\!\bullet\!\!-\!\!\bullet_{\beta}$ to $\bullet\!\!-\!\!\bullet$, we can replace Eq. (3.101) by the equivalent expression

(3.102)

for which the numerical value of the diagram is calculated as

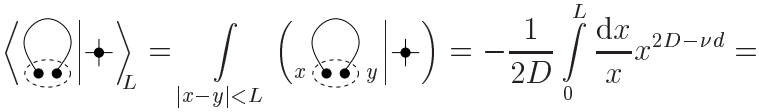

(3.103)

We can now subtract this term in a minimal subtraction scheme (MS). The internal dimension of the membrane D is kept fixed and (3.103) is expanded as a Laurent series in ε, which here starts at ε^{-1}. Denoting by $\langle\ |\ \rangle_{\varepsilon^p}$ the term of order ε^p of the Laurent expansion of $\langle\ |\ \rangle_L$ for $L = 1$, the residue of the pole in Eq. (3.103) is found to be

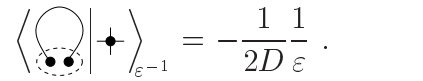

(3.104)

We shall also frequently employ the notation for the residue

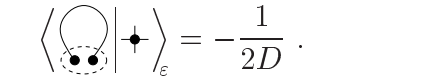

(3.105)

It is this pole that is subtracted in the MS-scheme by adding to the Hamiltonian a counter-term

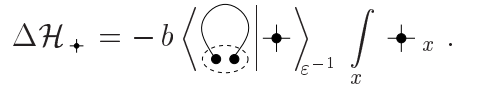

(3.106)

Note that by going from Eq. (3.101) to Eq. (3.106), we have reduced the integral counter-term to a number. We recall our initial remark that if one wants to check that this counter-term renders the theory finite, one should think of it as its defining integral

(3.101), and verify that in the resulting perturbation theory, the first-order divergence is absent.

Similarly, the divergence arising from the contraction of two dipoles to a single dipole is subtracted by a counter-term

$$\Delta\mathcal{H}$$  $$= b^2\mu^{2\varepsilon}$$ 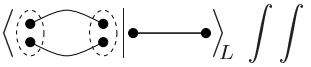 $$\int_x \int_y$$  $$, \qquad (3.107)$$

with

 $$. \qquad (3.108)$$

Reducing this integral counter-term to a number, we subtract the residue of the single pole of

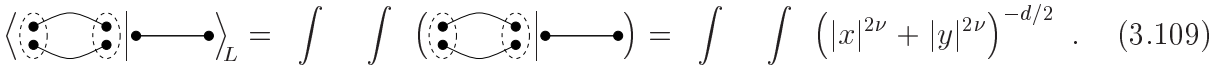

$$= \int_{|x|<L} \int_{|y|<L} \left(|x|^{2\nu} + |y|^{2\nu}\right)^{-d/2} . \qquad (3.109)$$

Note that the regulator L cuts off both integrations. One can now either utilize some simple algebra or show by the methods of conformal mapping (see section 4.3) that the residue is obtained by fixing one distance to equal 1 and by freely integrating over the remaining one

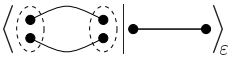 $$= \int_0^\infty \frac{\mathrm{d}x}{x} x^D \left(1 + x^{2-D}\right)^{-2D/(2-D)} . \qquad (3.110)$$

(Recall that $d/2 = 2D/(2-D) + O(\varepsilon)$.) The above is easily related to Euler's B-function and reads

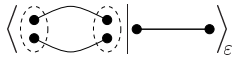 $$= \frac{1}{2-D} \frac{\Gamma\left(\frac{D}{2-D}\right)^2}{\Gamma\left(\frac{2D}{2-D}\right)} . \qquad (3.111)$$

As a result, the model is UV-finite at 1-loop order, if we use in the renormalized Hamiltonian (3.93) the renormalization factors Z and Z_b

$$Z = 1 - (2-D)$$ 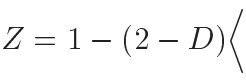 $$\frac{b}{\varepsilon} + O(b^2) \qquad (3.112)$$

$$Z_b = 1 +$$ 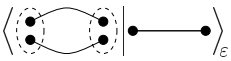 $$\frac{b}{\varepsilon} + O(b^2) . \qquad (3.113)$$

Note that due to Eq. (3.92) no counter-term for  is necessary.

The renormalized field and coupling are re-expressed in terms of their bare counterparts through

$$r_0(x) = Z^{1/2}\, r(x) , \qquad b_0 = b\, Z_b\, Z^{d/2}\, \mu^\varepsilon . \qquad (3.114)$$

Finally, the renormalization group functions are obtained from the variation of the coupling constant and the field with respect to the renormalization scale μ, keeping the bare

coupling fixed. (For a derivation, see appendix A.4). The flow of the coupling is written in terms of Z and Z_b as

$$\begin{aligned}\beta(b) &:= \mu\frac{\partial}{\partial\mu}\Big|_{b_0} b = \frac{-\varepsilon b}{1 + b\frac{\partial}{\partial b}\ln Z_b + \frac{d}{2}b\frac{\partial}{\partial b}\ln Z} \\ &= -\varepsilon b + \left(\left\langle \right|\!\bullet\!\!-\!\!-\!\!\bullet\!\left\rangle_\varepsilon - \nu d \left\langle \right|\!\bullet\!\left\rangle_\varepsilon \right) b^2 + O(b^3) \\ &= -\varepsilon b + \left(\frac{1}{2-D}\frac{\Gamma\left(\frac{D}{2-D}\right)^2}{\Gamma\left(\frac{2D}{2-D}\right)} + \frac{(2-D)d}{4D} \right) b^2 + O(b^3)\ . \end{aligned} \tag{3.115}$$

Similarly, the full dimension of the field (the exponent entering into the correlation function) is obtained as

$$\begin{aligned}\nu(b) &:= \frac{2-D}{2} - \frac{1}{2}\mu\frac{\partial}{\partial\mu}\Big|_{b_0} \ln Z = \frac{2-D}{2} - \frac{1}{2}\beta(b)\frac{\partial}{\partial b}\ln Z \\ &= \frac{2-D}{2}\left[1 - b\left\langle \right|\!\bullet\!\left\rangle_\varepsilon\right] + O(b^2) \\ &= \frac{2-D}{2}\left[1 + b\frac{1}{2D}\right] + O(b^2)\ . \end{aligned} \tag{3.116}$$

Note that minimal subtraction is used on the level of counter-terms or equivalently Z-factors. Since Z enters as Z^d into the β-function, the latter also contains a factor of d in the 1-loop approximation, i.e. Z^d is not minimally renormalized. In order to calculate the leading order in ε, the factor of d can be replaced by $d_c = \frac{4D}{2-D}$.

The β-function has a non-trivial fixed-point with $\beta(b^*) = 0$, which has positive slope and thus describes the behavior of the model at large distances:

$$b^* = \frac{\varepsilon}{\frac{1}{2-D}\frac{\Gamma\left(\frac{D}{2-D}\right)^2}{\Gamma\left(\frac{2D}{2-D}\right)} + 1} + O(\varepsilon^2)\ . \tag{3.117}$$

The anomalous dimension $\nu^* := \nu(b^*)$ becomes to first order in ε

$$\nu^* = \frac{2-D}{2}\left[1 + \frac{\varepsilon}{2D}\frac{1}{\frac{1}{2-D}\frac{\Gamma\left(\frac{D}{2-D}\right)^2}{\Gamma\left(\frac{2D}{2-D}\right)} + 1}\right] + O(\varepsilon^2)\ . \tag{3.118}$$

For polymers, this result reduces to the well-known formula

$$\nu^*(D=1) = \frac{1}{2} + \frac{4-d}{16} + O((4-d)^2)\ . \tag{3.119}$$

3.9 Non-renormalization of long-range interactions

Long-range interactions are in general not renormalized [56]. This is very useful, as it immediately enforces scaling relations among the critical exponents, which in some cases are already sufficient to determine these exponents. Let us explain the non-renormalization by analyzing the long-range interaction ($\alpha > 0$)

$$= \int_k |k|^{-\alpha} \mathrm{e}^{ik[r(x)-r(y)]}$$
$$\sim |r(x) - r(y)|^{\alpha-d} \tag{3.120}$$

Then the most simple singular configurations which give rise to a renormalization of the interaction are those for which two interactions are contracted to a single one, as we have discussed in 3.5. We claim that their multilocal operator product expansion (MOPE),  , does not contain a contribution proportional to  , but that the leading term is proportional to the short-range interaction  . This is a consequence of the analytic structure of the long-range interaction: The contraction  is in complete analogy to Eq. (3.87) and with the same notations as there

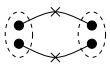

$$= \int_k \int_p |k|^{-\alpha} |p|^{-\alpha} \mathrm{e}^{i(k+p)[r(x)-r(y)]} \mathrm{e}^{kp[C(u)+C(v)]}$$
$$+ \text{subdominant terms} \; . \tag{3.121}$$

In order to obtain a long-range term, a singularity at $k + p = 0$ is necessary. However, expression (3.121) is analytic at $k + p = 0$, and no long-range term is generated. This is easily generalized to any contraction towards and hence to any order in perturbation theory.

Let us now analyze the consequences. We want to study tethered membranes with long-range interactions, generalizing Eq. (3.1) or Eq. (3.93) to

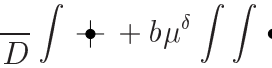

$$\mathcal{H}_{\mathrm{LR}} = \frac{Z}{2-D} \int_x \; + \; + b\mu^\delta \int_x \int_y \; .$$
(3.122)

Note that since in contrast to Eq. (3.1) the interaction is not renormalized, there is only one Z-factor in Eq. (3.122), namely for elasticity. This does, however, not mean that the β-function is trivial. In analogy to Eq. (3.114), the relation between bare and renormalized coupling is

$$b_0 = b Z^{(d-\alpha)/2} \mu^\delta \; , \tag{3.123}$$

where Z is as in Eq. (3.114) the renormalization of the field, and

$$\delta = 2D - \nu(d - \alpha) \; . \tag{3.124}$$

The β-function now reads

$$\beta(b) = \mu \frac{\partial}{\partial \mu}\bigg|_{b_0} b = \left[-\delta + \frac{\alpha - d}{2} \mu \frac{\partial}{\partial \mu} \ln Z \right] b \; . \tag{3.125}$$

Using the fact that $\mu\frac{\partial}{\partial\mu}\ln Z$ is nothing but (-2) times the anomalous dimension of the field, see Eq. (3.116), we make the replacement

$$\mu\frac{\partial}{\partial\mu}\ln Z = 2(\nu - \nu(b)) \tag{3.126}$$

in Eq. (3.125). The result is

$$\beta(b) = -\left[2D - (d-\alpha)\nu(b)\right] b \ . \tag{3.127}$$

This β-function has to zeros: For $\delta < 0$, the fixed point at $b^* = 0$ is attractive. For $\delta > 0$ the non-trivial zero and fixed point of $\beta(b)$ is at $b^* > 0$, implying the exponent-identity

$$\nu^* = \nu(b^*) = \frac{2D}{d-\alpha} \ . \tag{3.128}$$

Non-renormalization of the coupling thus allows to obtain ν^* without calculating any diagram. Since this observation is quite generally useful, let us give a heuristic derivation of Eq. (3.128). We may then consider the formal derivation given above as a proof of the heuristic argument, and employ the latter confidently throughout this review.

"Power counting" for the dimension $\mathcal{D}$ of the interaction at a fixed point yields

$$\mathcal{D} = 2D - \nu^*(d-\alpha) \ , \tag{3.129}$$

and this power-counting gives the correct dimension of the operator, since the latter has no proper renormalization. Three different scenarios are now possible: If $\mathcal{D} < 0$, then the associated coupling scales to 0, and the operator plays no role in the large scale limit. If $\mathcal{D} > 0$, then the associated coupling grows under renormalization and we are *not* at an IR-fixed point; by definition this is not the situation considered here. The last possibility is that we are at an IR-fixed point, and this is (at least for one coupling) equivalent to $\mathcal{D} = 0$. It again follows the exponent identity

$$\nu^* = \nu(b^*) = \frac{2D}{d-\alpha} \ . \tag{3.130}$$

Also the crossover from short-range to long-range self-avoidance in a model with both couplings can be discussed in this framework. Following the line of arguments given above, long-range self-avoidance will scale to 0 and the short-range fixed point is completely attractive as long as $\mathcal{D}$, Eq. (3.129), evaluated with ν^* as obtained from short-range self-avoidance only, is negative. As a consequence always that interaction wins, which yields the larger value for ν^*.

Physically, long-range forces play an important role for charged membranes, as discussed in [150].

4 Some useful tools and relation to polymer theory

4.1 Equation of motion and redundant operators

The equation of motion reflects the invariance of the functional integral under a global rescaling of the field r. This has important consequences. Consider the expectation value